Localization, superconducting fluctuations, and superconductivity in thin films and narrow wires of aluminum

P. Santhanam,* S. Wind, and D. E. Prober
Section of Applied Physics, Yale University, P.O. Box 2157, New Haven, Connecticut 06520
(Received 2 July 1986)

We report a comprehensive set of experiments on wide and narrow thin-film strips of aluminum which test the predictions of recent localization theory. The experiments on wide films in the two-dimensional regime confirm the theoretical predictions and also yield insight into inelastic mechanisms and spin-orbit scattering rates. Our extension of the existing theory for one-dimensional systems to include spin-orbit scattering and Maki-Thompson superconducting fluctuations is verified by the experiments. We find clear evidence for one-dimensional localization, with inferred inelastic rates identical to those in two-dimensional films. The prediction of the localization theory for a dimensional crossover from two-dimensional to one-dimensional behavior is also confirmed. We have reanalyzed the results of some previous experiments on thin films and narrow wires in light of these results.

I. INTRODUCTION

Since the theoretical prediction of electron localization effects by Thouless[1] and the scaling theory proposed by Abrahams *et al.*,[2] many experiments have been carried out to verify these predictions in metal films[3] and metal-oxide-semiconductor field-effect transistors (MOSFET's).[4] Early experiments attempted to test the predictions of localization theory by studying the behavior of the resistance as a function of temperature. However, other quantum effects, due to electron-electron interactions,[5] made the interpretation of the experimental $R(T)$ data nontrivial. Microscopic calculations have since shown that the magnetoresistance at small magnetic fields can be used to separate the localization contribution from the interaction contribution,[6] and subsequent experiments have concentrated on magnetoresistance studies.

In recent years studies of normal-metal films and MOSFET's have confirmed many of the predictions of the localization theory; important parameters of relevance to electron transport have been inferred. A review of the conclusions on nonsuperconducting metal films can be found in Ref. 3. In most cases the inferred inelastic scattering rates were found to be too large to be explained by known inelastic mechanisms, such as electron-electron scattering or electron-phonon scattering. Following the calculations of magnetoresistance by Larkin[7] for Maki-Thompson superconducting fluctuations, experiments on superconducting films for $T \gg T_c$ could also be successfully interpreted. Studies on aluminum films have been particularly fruitful with respect to yielding understandable inelastic rates. In this article, we synthesize and review our recent work on thin films and narrow wires of aluminum. Some of this work has been published previously as four short papers.[8–11] The purpose of this article is to present the various results of our experiments that test many aspects of the modern localization theory in a coherent way. We present these results in some detail because aluminum films and wires have proven to be near ideal material systems. Stable Al films with reproducible properties are easily prepared. Also, common magnetic impurities do not possess magnetic moments in Al, thus considerably simplifying the interpretation of the inferred results. In addition, the inelastic scattering time (τ_i) in Al is long, implying longer times for observing phase coherence necessary for localization. Aluminum is therefore a good candidate for studies of quantum transport. Our work provides an important basis for such studies. Further details on this article can be found in Ref. 12.

This paper is organized as follows. In Sec. II we discuss the relevant theoretical predictions for quasi-two-dimensional and quasi-one-dimensional systems. The scattering mechanisms responsible for electron delocalization and some aspects of spin-orbit scattering are also briefly outlined. Section III describes the experimental details of sample fabrication and measurement techniques. Data analysis and comparison to theory are given in Sec. IV. In Sec. V we compare our results to those of other experiments, and in Sec. VI we summarize our conclusions.

II. THEORY

The theory of quantum corrections to the electrical resistance at low temperatures, as relevant to superconducting films above T_c, has been summarized by Bergmann.[13] There are *six* contributions which add to the classical Drude resistance at low temperatures. These contributions arise from: (i) localization effects; (ii) Maki-Thompson superconducting fluctuations; (iii) Aslamazov-Larkin superconducting fluctuations; (iv) electron-electron Coulomb interaction; (v) classical electron-phonon scattering; and (vi) classical magnetoresistance. The clean nature of our films (due to relatively long elastic mean free paths) makes the localization and Maki-Thompson (MT) contributions dominate over the other two quantum contributions, (iii) and (iv) above. We can safely ignore the Aslamazov-Larkin term in our work, since our experiments are done in the regime

$(T/T_c) > 1.3$. Electron-electron interaction effects can be ignored as long as $\tau_i \gg \hbar/k_B T$. We refer the reader to Bergmann[13] for an account of the contributions from Aslamazov-Larkin fluctuations and electron-electron interactions (both particle-particle and particle-hole types). In our experiments the elastic scattering time $\tau \ll \tau_i$, and hence classical electron-phonon scattering contributes directly only to the temperature dependence of the resistance, but not to the magnetoresistance (MR). We discuss in this section, only the two dominant quantum corrections, viz. localization and MT fluctuations, in detail. The classical magnetoresistance and the electron-phonon contribution to the temperature resistance are outlined in Sec. II C.

The localization effect is due to the coherence between time-reversally related impurity scattered waves of a single electron.[3] The two interfering electron waves have nearly equal and opposite momenta, resulting in a stationary state.[14] Inelastic electron scattering mechanisms (such as electron-phonon scattering or electron-electron scattering) limit the time over which this phase coherence can last. In principle, this phase coherence time can be different from the inelastic scattering time for single electrons (quasiparticles). In our discussion below we use "inelastic" to imply "a process destroying the phase coherence of the localized electron state." As we shall see from our experimental results, the phase coherence time appears to differ from the quasiparticle inelastic scattering time only by a multiplicative factor of order unity.

In the original theoretical work by Thouless[1] the length determining sample dimensionality for localization effects was taken to be the inelastic diffusion length $l_i = (D\tau_i)^{1/2}$; D is the diffusion constant. Spin-orbit scattering was *not* included in that theory. The spin-orbit Hamiltonian does not violate the time-reversal symmetry of impurity scattering events.[15] It is now known[3,16] that when spin-orbit scattering is present, the coherence required for the interference is not destroyed, but the amplitude of the interference is modified due to spin matrix elements. In such a situation, there is a second length scale for deciding the localization dimension given by

$$l_2 = (D\tau_2)^{1/2} .$$

where $\tau_2^{-1} = \tau_i^{-1} + \frac{4}{3}\tau_{\text{s.o.}}^{-1}$. $\tau_{\text{s.o.}}$ is the characteristic time that corresponds to spin-orbit scattering.

The physical origin[17] of the MT fluctuation term is due to the correlated *pair of quasiparticles* of near-zero total momentum that result from the decay of a superconducting fluctuation at $T > T_c$. Time-reversal symmetry is also required for maintaining the correlation between these two quasiparticles of near-zero total momentum that give rise to the excess MT conductivity. The MT term is *not* affected by spin-orbit scattering since the spin-orbit Hamiltonian does not violate time-reversal symmetry and the superconducting pairing involves time reversally related states. It appears[7] that the same phase-relaxation time is appropriate for both the MT and localization terms. The length scale for deciding the dimensionality for MT fluctuations is the inelastic scattering length l_i.

We note also that magnetic impurities destroy both the localization and the MT fluctuation contributions. In this article, we take the *magnetic scattering to be negligible.* For the case of Al, this assumption of negligible magnetic scattering is well justified. This is because in dilute concentrations, common magnetic impurities do not have localized magnetic moments in Al.[18] However, all of our theoretical expressions for the *localization contribution* can be generalized[3] to include the magnetic scattering rate τ_s^{-1} by substituting $\tau_i^{-1} + 2\tau_s^{-1}$ for τ_i^{-1}, and $\tau_i^{-1} + \frac{4}{3}\tau_{\text{s.o.}}^{-1} + \frac{2}{3}\tau_s^{-1}$ for τ_2^{-1}.

For all the discussions which follow, the *magnetoresistance* at a temperature T is defined as

$$\frac{\delta R}{R} = \frac{\Delta R(T,H) - \Delta R(T,H=0)}{R} , \tag{1}$$

where ΔR is a given contribution (or sum of contributions) to the resistance at a *fixed temperature* T and at a *fixed field* H. The resistance change as a function of temperature, in a field H, is defined as

$$\frac{\delta \tilde{R}}{R} = \frac{\Delta R(T,H) - \Delta R(T_{\text{ref}},H)}{R} . \tag{2}$$

A. Two-dimensional systems: Quantum corrections to the resistance

We consider the films two-dimensional when the film thickness $d \ll l_i$ and l_2. We are interested in studying the electrical resistance in a static magnetic field. We give theoretical results for two-dimensional systems for two field orientations: (i) perpendicular to the plane of the film, and (ii) parallel to the plane of the film. Most experiments are done in the perpendicular field orientation.

1. Perpendicular fields

a. Localization. The fractional change in resistance due to localization at a given temperature T and magnetic field H is[6,19]

$$\frac{\Delta R^{\text{loc}}}{R}(T,H) = \frac{R_\square}{2\pi^2\hbar/e^2}\left[-\frac{3}{2}\psi\left(\frac{1}{2}+\frac{H_2}{H}\right) + \frac{1}{2}\psi\left(\frac{1}{2}+\frac{H_i}{H}\right) + \ln\frac{H_0}{H}\right] \tag{3a}$$

$$= \frac{3}{2}f_2(H,H_2) - \frac{1}{2}f_2(H,H_i) \tag{3b}$$

with

$$f_2(H,H_i) = -(e^2R_\square/2\pi^2\hbar)[\psi(\tfrac{1}{2}+H_i/H) - \ln(H_0/H)] .$$

Here $R_\square$ is the sheet resistance of the film $H_2 = H_i + \frac{4}{3}H_{\text{s.o.}}$, $H_i = \hbar c/4eD\tau_i$, $H_{\text{s.o.}} = \hbar c/4eD\tau_{\text{s.o.}}$, and $H_0 = \hbar c/4eD\tau$. ψ is the digamma function. D $(= v_F l/3)$ is the three-dimensional diffusion constant. τ_i the inelastic lifetime, $\tau_{\text{s.o.}}$ the spin-orbit scattering time, and τ the elastic scattering time. v_F is the Fermi velocity. Each characteristic field H_x corresponds to the relevant scattering rate τ_x^{-1}. In the absence of a magnetic field, the elastic mean free path, $l = v_F\tau$, is taken to be the shortest

length over which the coherence required for localization is possible. [Note that $\psi(\frac{1}{2}+u)\rightarrow \ln u$ as $u\rightarrow\infty$.]

b. Maki-Thompson fluctuations. The contribution to the fractional resistance change due to Maki-Thompson (MT) superconducting fluctuations is given for fields such that $H \ll (ck_BT/4De)\ln(T/T_c)$ and $\hbar/\tau_i \ll k_BT\ln(T/T_c)$ by,[7]

$$\frac{\Delta R^{\mathrm{MT}}}{R}(T,H) = -\frac{R_\square}{2\pi^2\hbar/e^2}\beta(T/T_c)\psi\left[\frac{1}{2}+\frac{H_i}{H}\right] . \quad (4)$$

$\beta(T/T_c)$ is the parameter introduced by Larkin[7(a)] to characterize the interaction between electrons. β is independent of localization dimensionality and it diverges as $T\rightarrow T_c$. As seen in Eq. (4), the role of inelastic scattering events in depressing the MT term is strikingly similar to the effect on the singlet localization term [the term with the prefactor $\frac{1}{2}$ in Eq. (1)]. For $H \ll H_i$ *and* $H \ll (ck_BT/4De)\ln(T/T_c)$ (and hence for zero field) one should use[7(b),16]

$$\frac{\Delta R^{\mathrm{MT}}}{R}(T,H=0) = \frac{R_\square}{2\pi^2\hbar/e^2}\beta(T/T_c)\ln\left[\frac{8k_BT\ln(T/T_c)\tau_i}{\pi\hbar}\right] . \quad (5)$$

This result is due to the fact that the cutoff energy in the calculation of the MT term is $k_BT\ln(T/T_c)$. This differs from the cut-off $\hbar/\tau$ in the localization calculation.

2. Parallel fields

a. Localization. When the magnetic field is parallel to the plane of the film only a perturbation calculation for the localization contribution is available.[20] The theoretical result for this contribution to the fractional resistance change due to localization is[21]

$$\frac{\Delta R^{\mathrm{loc}}}{R} = \tfrac{3}{2}f_{2\|}(H,H_2) - \tfrac{1}{2}f_{2\|}(H,H_i) , \quad (6)$$

where

$$f_{2\|}(H,H_i) = -\frac{R_\square}{2\pi^2\hbar/e^2}\left[\ln\left[\frac{H_i}{H_0}\right]+\ln\left[1+\frac{H^2}{48H_iH_d}\right]\right],$$

with $H_d = \hbar c/4ed^2$.

b. MT fluctuations. The contribution to the fractional resistance change due to MT fluctuations at a fixed T and at a finite field H is[21]

$$\frac{\Delta R^{\mathrm{MT}}}{R} = -\beta(T/T_c)f_{2\|}(H,H_i) . \quad (7)$$

The magnetoresistance is again obtained from Eq. (1).

From the calculations of Saint-James and de Gennes[22] on the nucleation of superconductivity in a thin film in a parallel magnetic field, it is possible to give an upper limit for the field beyond which the small field approximation leading to Eqs. (6) and (7) breaks down. This is because the equations for the superconducting order parameter in the linearized Ginzburg-Landau theory and the wave function describing coherence in the localization theory have the same form.[9,12] As indicated in Ref. 9, this implies that the perturbation result is valid only for small fields,[12] $H < 12H_d$. As expected, this condition corresponds approximately to fields for which the size of the lowest Landau level, $l_H = (\hbar c/2eH)^{1/2}$, is larger than the film thickness d.

B. Narrow wires: Quantum corrections to the resistance

The one-dimensional localization theory is applicable[9] when the sample width W and thickness d are smaller than the inelastic scattering length l_i, and the effective scattering length l_2. We call this the *fully-one-dimensional* (fully-1D) regime. Since $l_{\mathrm{s.o.}}$ and hence l_2 can be as small as a few hundred Å in many metals, most of the early experiments on narrow wires of width $\gtrsim 500$Å were not in the fully-1D regime. The likely experimental situation for many of those wires studied in the early experiments was that $l_2 < W < l_i$. We call this the regime of *mixed dimensionality,* as explained in the discussion below. We discuss our (re)interpretation of the early experimental studies on wires in Sec. V, at the end of this paper.

As in the case of the 2D systems, we discuss in detail only the localization and MT terms. We will give results for an experimental geometry which is a flat strip of width W. We take the magnetic field to be normal to the film. [See Fig. 1(d) below].

1. Fully-one-dimensional systems

a. Localization. We have recently reported[9] our extension of the original 1D calculation of Alt'shuler and Aro-

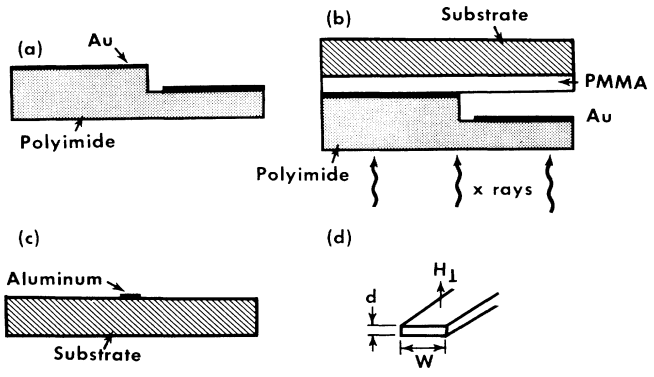

FIG. 1. (a)—(c) describe the steps in the fabrication of narrow wires using x-ray lithography. (a) Gold x-ray absorber pattern formed by evaporating Au over a reactive-ion etched step in polyimide (side view). (b) PMMA is exposed by x-ray photons. Mask and substrate are held in contact electrostatically. (c) Aluminum is evaporated onto developed PMMA pattern and "lifted-off," leaving a narrow wire whose width is determined by the gap in the x-ray mask. (d) Experimental geometry for the magnetoresistance measurements on narrow wires.

nov[20] for the 1D localization magnetoresistance to include the effects of spin-orbit scattering. With spin-orbit scattering present, the localization contribution to the normalized resistance at fixed T and H is

$$\frac{\Delta R^{\rm loc}}{R}(T,H)=\tfrac{3}{2}f_1(H,H_2)-\tfrac{1}{2}f_1(H,H_i)\ , \tag{8a}$$

where

$$f_1(H,H_i)=\frac{R_\Box}{\pi\hbar/e^2}\left[\frac{H_W}{H_i}\right]^{1/2}\left[1+\frac{H^2}{48H_iH_W}\right]^{1/2}. \tag{8b}$$

The form of Eq. (8b) also applies for $f_1(H,H_2)$. In Eq. (8a), the first term is the "triplet" part of the Cooper-propagator contribution and the second term is the "singlet" part. The triplet part is sensitive to spin-orbit scattering; the singlet part is not. When spin-orbit scattering is negligible ($\tau_{\rm s.o.}\to\infty$), we obtain the result of Alt'shuler and Aronov. The derivation of Eq. (8) involves the use of perturbation theory as in the derivation of Eq. (6). Therefore, for Eq. (8) the field restriction is $H<12H_W$ ($H_W=\hbar c/4eW^2$), since it is the width of the wire which is to be compared to the Landau orbit size $l_H=(\hbar c/2eH)^{1/2}$.

b. Maki-Thompson fluctuations. Since the scaling length for the MT fluctuations is the inelastic scattering length, the behavior of the MT contribution is 1D when $W<l_i$. For $H\ll(ck_BT/4De)\ln(T/T_c)$ and $\hbar/\tau_i\ll k_BT\ln(T/T_c)$ we obtain[9,12]

$$\frac{\Delta R^{\rm MT}}{R}(T,H)=-\beta(T/T_c)f_1(H,H_i)\ . \tag{9}$$

The magnetoresistance can be calculated as before. The choice for the cutoff energy does not appear explicitly in the 1D results [Eq. (8) and Eq. (9)] because of our assumptions that $\tau\ll\tau_i$ and $\hbar/\tau_i\ll k_BT\ln(T/T_c)$, respectively. Very recently, this theory has been extended to lower temperatures and higher magnetic fields.[23]

2. Mixed-dimensional systems

When $l_2\ll W\ll l_i$, the wire is in the mixed-dimensional regime for the localization contribution, as noted above. The triplet contribution is two-dimensional since $(D\tau_2)^{1/2}<W$ and $l_2=(D\tau_2)^{1/2}$ is the length scale determining sample dimensionality for the triplet term. The singlet contribution is one-dimensional. In this case,[9,12]

$$\frac{\Delta R^{\rm loc}}{R}=\tfrac{3}{2}f_2(H,H_2)-\tfrac{1}{2}f_1(H,H_i)\ . \tag{10}$$

We note that in this mixed-dimensional regime the triplet contribution is small compared to the singlet contribution. In this case, *positive* magnetoresistance, called antilocalization by Bergmann,[3] will result. When the spin-orbit rate is *very* large compared to the inelastic rate, the singlet term alone is adequate for interpretation of the data. We expect that a sample which shows mixed-dimensional behavior at low temperatures will have two-dimensional behavior at high temperatures, since at high temperatures l_i will also be less than W.

For the contribution due to MT fluctuations, l_i is the only relevant length scale. Thus, the MT contribution is identical to the fully-1D result given by Eq. (9).

C. Classical contributions to the resistance

The localization and MT contributions are the dominant quantum corrections to the resistance for our samples. There are two "classical" contributions which are also significant for both the wires and films. These are (1) the electron-phonon contribution to the resistance as function of temperature, and (2) classical magnetoresistance. These classical contributions are important because our samples are relatively clean: $k_Fl\gg1$ and $R_\Box\sim1\ \Omega$. (k_F is the Fermi wave vector.) Classical contributions to $R(T,H)$ are generally not discussed in studies of localization because much dirtier systems ($k_Fl\sim1$) are usually studied. In these dirtier systems the quantum contributions alone dominate.

The standard result for the electron-phonon contribution to $R(T)$ due to phonon scattering is the Bloch-Gruneissen law.[18] This result is that $\Delta R^{\rm ph}\propto T^5$ for $T\ll\Theta_D$. This T^5 form is due to the restriction to small-angle electron scattering by phonons at low temperatures. This restriction leads to multiplying the electron-phonon scattering rate, $\propto T^3$, by an additional T^2 factor which reflects the average amount by which the electron's forward momentum is decreased by a phonon scattering event.[18] For aluminum, previous experiments indicate that[24]

$$\Delta R^{\rm ph}\propto T^3\ . \tag{11}$$

This T^3 behavior results essentially from the large amount of umklapp scattering, wherein the electron velocity (and momentum) can change by a large amount for a small change in k. As we shall see in Sec. IV, our results find the same T^3 behavior as found in bulk Al samples.[24]

The effect of a magnetic field on the electron orbits in solids is discussed in many textbooks.[18] In the case when τ is much shorter than τ_i, one expects the classical magnetoresistance to be *temperature independent.* We note that the free-electron theory of metals does not predict any magnetoresistance.[18] Using a more realistic two-band model[12,18] for aluminum (due to the electron and hole bands) one obtains a result,

$$\frac{\delta R^{\rm cl}}{R}=b\,(Hl)^2\propto(\omega_c\tau)^2\ , \tag{12}$$

for $\omega_c\tau\ll1$ (ω_c is the cyclotron frequency, eH/mc) with a value $b\sim0.25$ estimated using reasonable band structure parameters.[12] In our samples, $(\omega_c\tau)$ is small, $\sim10^{-4}$ at 1 kG. The experimental results in Sec. IV qualitatively confirm the behavior expected for the magnetoresistance.

D. Inelastic scattering mechanisms

Only recently has there been some significant progress in our understanding of the inelastic processes that result in the delocalization of electrons. We discuss in some detail two inelastic mechanisms we believe to be relevant in our experiments. We will note, where necessary, the difference between the inelastic processes which relax the

energy of a *single* electron (quasiparticle), and those processes which break the coherence required for localization.

1. Electron-phonon scattering

Electron-phonon scattering is the only well studied inelastic mechanism in pure metals. In the case of impure metals, some early theoretical calculations on electron-phonon scattering have also been performed using simple models. Prior to the recent localization studies on Al, there was no quantitative evidence for electron-phonon inelastic scattering in any of the localization studies.

The dimensionality of a system with respect to electron-phonon scattering is generally decided[25] by comparing the physical dimensions of the system to the most probable phonon wavelength, $\lambda_{\rm ph}=2\pi/q_{\rm ph}$. $q_{\rm ph}$ is the characteristic phonon wave vector $=2k_BT/(v_s\hbar)$, with v_s the velocity of sound. For Al, transverse phonons give the major contribution to inelastic scattering[26] and for these, $\lambda_{\rm ph}=750$ Å$/T$, with T in K. If one uses, instead, the Pippard-Ziman condition[27] that phonons of wavelength larger than the electron mean free path are inefficient scatterers, then the electron mean free path will determine the dimensionality of electron-phonon scattering. With either criterion, we estimate that our samples are in the regime of *three-dimensional* electron-phonon scattering for the temperature range where electron-phonon scattering dominates, typically >5 K. The good adhesion of the film to the substrate and the good acoustic impedance match of Al and the glass substrate further enhance the three dimensionality of this scattering mechanism.

Lawrence and Meador have calculated the electron-phonon scattering rate in aluminum[26] using microscopic band-structure parameters and realistic electronic wave functions. They obtained a value for the electron-phonon inelastic rate for quasiparticles in clean, bulk Al at the Fermi energy:[26]

$$\tau_{e\text{-ph}}^{-1}=(0.9\times10^7)T^3=A_3^{\rm theor}T^3\ . \tag{13}$$

This rate is an average over the Fermi surface of $\tau_{e\text{-ph}}^{-1}(\mathbf{k})$, as is appropriate for our polycrystalline films. A number of experiments on bulk single-crystal Al measured $\tau_{e\text{-ph}}^{-1}(\mathbf{k})$ at specific points or averaged on specific orbits on the Fermi surface.[26] These experiments confirm the magnitude and $\mathbf{k}$ dependence of the prediction by Lawrence and Meador for $\tau_{e\text{-ph}}^{-1}$. The prediction of Eq. 13 for a Fermi-surface-averaged rate may thus be used reliably for quantitative comparison with our experimental results, which deal with polycrystalline films. It is likely[28] that the phase-relaxation rate relevant for localization due to electron-phonon scattering will be close to the *quasiparticle* inelastic rate for electron-phonon interactions.

For clean-limit ($q_{\rm ph}l>1$) electron-phonon scattering in bulk (3D) samples there is general theoretical consensus that $\tau_{e\text{-ph}}^{-1}$ should go as T^3. The expected behavior for dirty-limit ($q_{\rm ph}l<1$) electron-phonon scattering is still in controversy. A rate proportional to T^4 has been predicted by Schmid[29] and by Thouless.[1] Two different theoretical calculations by Takayama[30] and by Kagan and Zhernov[31] predict an electron-phonon rate in dirty systems proportional to T^2. The behavior is likely more complicated than that of a single power law (T^p) for the range of temperatures and mean free paths which are used in actual experiments.[28] In addition, all the dirty-limit calculations[28,30,31] to date are for metals with a spherical Fermi surface. In this simple model, an important consequence of the decrease in the elastic mean free path is that inelastic scattering by transverse phonons in addition to the usual scattering by longitudinal phonons[28] is allowed. However, in real metals, and specifically aluminum, the electron wavefunctions are such that the transverse phonons already cause $\sim80\%$ of the inelastic scattering even in pure, bulk samples.[26] Thus, the calculations for idealized metals with free-electron wave functions and spherical Fermi surfaces probably do *not* provide useful guidance regarding dirty-limit electron-phonon scattering in metals such as Al. In any case, our samples are in the clean regime ($q_{\rm ph}l>1$) in the temperature range where electron-phonon scattering is the dominant mechanism.

2. Electron-electron scattering

The standard result for the electron-electron scattering rate in clean systems is a rate proportional to T^2 (see, e.g., Ref. 18). This T^2 rate applies only for clean ($\hbar/\tau<k_BT$), bulk (i.e., three-dimensional) systems. The quasiparticle electron-electron lifetime in clean bulk Al (using its detailed band structure) has been calculated by Lawrence and Wilkins[32(a)] and modified by MacDonald.[32(b)] There have also been calculations by Schmid[29] for dirty ($\hbar/\tau>k_BT$) systems. We note that the theory of electron-electron scattering in the dirty limit, incorporating the bandstructure of Al, is not available. Hence we compare our experimental results to theoretical predictions based on simple models of metals with a spherical Fermi surface.

Abrahams *et al.*[33] have calculated the electron-electron inelastic *quasiparticle* scattering rate for dirty *two-dimensional* systems. The characteristic length scale for dirty electron-electron inelastic interactions is $l_{\rm int}=(\hbar D/k_BT)^{1/2}$. When $d\ll l_{\rm int}$ they obtained for the *quasiparticle* inelastic rate

$$\tau_{ee}^{-1}=\frac{e^2R_\square}{2\pi\hbar^2}k_BT\ln(T_1/T)\ , \tag{14}$$

with[8] $T_1=(9\times10^5)(k_Fl)^3\sim10^{12}$ for Al. Thus, $\ln(T_1/T)\sim25$. This result has been extensively used in the literature, including our previous publications.[8–11] Subsequently, Lopes dos Santos[34] reevaluated the quasiparticle rate self-consistently and obtained an expression for τ_{ee}^{-1} that is smaller than the rate predicted by Eq. (14) essentially by a factor of 2. Alt'shuler and Aronov[35] have predicted a similar result for the *quasiparticle* inelastic electron-electron rate, but without the logarithmic factor. Their rate is therefore much smaller than the result of Eq. (14).

Fukuyama and Abrahams[36] have evaluated explicitly the phase-relaxation time entering the weak localization problem due to the dynamically screened electron-electron interaction. They conclude that the phase-relaxation rate

τ_ϵ^{-1} for *2D systems* is given by the same expression, Eq. (14).

Alt'shuler *et al.*[16,37] (and recently Eiler[38]) have calculated the phase-relaxation rate for the weak localization correction due to electron-electron scattering at small energy ("quasielastic" scattering) transfers using a path integral approach. This result is equivalent to electron phase relaxation caused by electromagnetic fluctuations.[16,37] These calculations indicate that in reduced-dimensional systems (2D and 1D), the phase relaxation rate due to quasielastic processes (denoted in their work as τ_N^{-1}) can be large. Alt'shuler *et al.*[37] predict that phase-relaxation rate *for 2D systems* is given by

$$\tau_\epsilon^{-1}=\left[\frac{e^2R_\square}{2\pi\hbar^2}\right]k_BT\ln(\pi\hbar/e^2R_\square)$$
$$=A_1^{\text{theor}}T\sim(4\times10^7)R_\square T\ . \tag{15}$$

The condition for two-dimensional behavior required for the use of Eq. (15) is

$$d\ll l_{\text{int}}$$

and (15a)

$$d\ll\left[\frac{2\pi(\hbar/e^2)}{\rho_0}\left[\frac{\hbar D}{k_BT}\right]\frac{1}{\ln[\pi(\hbar/e^2)/R_\square]}\right]\ .$$

We note that Eq. (15) differs from Eq. (14) by the absence of the temperature dependence in the argument of the logarithm. In the case of 2D systems of low sheet resistance such as our thin films, this theoretical prediction for τ_ϵ^{-1} is smaller than that predicted by Fukuyama and Abrahams[36] by a factor of 3. Fukuyama[39] has attempted to relate the calculations of Alt'shuler *et al.*[37] to that of Fukuyama and Abrahams.[36] It appears[39] that the inelastic processes considered by these different authors arise from the same physical mechanism, though this is not evident in their papers. Our experimental samples are in the limit given by Eq. (15a). According to the recent conclusions of Fukuyama[39] (as also recently summarized by Abrahams[40]), it is the 2D prediction of Alt'shuler *et al.* given by Eq. (15) that correctly describes the decay rate of the phase coherence due to electron-electron interaction for two dimensional systems. Therefore, we use Eq. (15) for comparison to our experimental data. In *1D systems* τ_ϵ^{-1} is predicted by Alt'shuler *et al.* to be[16,37]

$$\tau_\epsilon^{-1}=\left[\frac{e^2R_\square k_BT}{\hbar^2W}\right]^{2/3}(D/2)^{1/3}\ , \tag{16}$$

where W is the width of the wire. The condition[16] for the use of Eq. (16) is that

$$W\ll\frac{(\hbar/e^2)}{R_\square\pi\sqrt{2}}\left[\frac{\hbar D}{k_BT}\right]^{1/2}\ .$$

This Cooper-propagator rate can be much larger than the 1D *quasiparticle* inelastic rate,[29(b),35], which is proportional to $T^{1/2}$.

Very recently, it has been pointed out[41] that in the case of superconducting samples, close to the superconducting transition, the electron-electron inelastic scattering rate can be modified due to superconducting fluctuations.[41] A complex dependence of τ_ϵ^{-1} on magnetic field and disorder is introduced by such a mechanism. For the lowest temperature used in our work such a theory would increase the theoretical estimate for τ_ϵ^{-1} by at most $\sim20\%$.

3. *Other inelastic mechanisms*

In the case of amorphous systems Black *et al.*[42] calculated the inelastic time due to the existence of two-level systems. Results of the early experiments on wires of highly disordered Au-Pd metal alloys[43] were compared with that prediction, since the data on Au-Pd wires seemed to indicate that $\tau_i^{-1}\propto T$. In Sec. V we discuss the method of data analysis which led to the conclusion that $\tau_i^{-1}\propto T$, and show that those conclusions on τ_i^{-1} must be revised. In any case, it is likely that this mechanism is *not* relevant for the relatively clean polycrystalline metal films we employ in the present studies.

E. Spin-orbit scattering

The origin of spin-orbit scattering in thin metal films has remained a puzzle for more than a decade.[44,45] In most experiments on electron transport, effects due to spin-orbit scattering are masked by the effects of other scattering processes. In addition, any theory of the spin-orbit scattering rate requires a good model of the impurity or defect scattering process(es). An estimate of the spin-orbit scattering rate in a metal using a simple scattering model was given by Abrikosov and Gorkov.[44] They predicted that

$$\tau/\tau_{\text{s.o.}}=(\alpha Z)^4\ , \tag{17}$$

where α is the fine structure constant ($\sim\frac{1}{137}$), and Z is the atomic number of the metal. It is indeed plausible that the spin-orbit scattering time should scale with the elastic scattering time, since it is the deviations from ideality (impurities, boundaries, and defects) that cause both elastic and spin-orbit scattering. For Al, $Z=13$, so that the ratio predicted by Eq. (17) is 0.8×10^{-4} if the elastic scattering of electrons is due to boundaries. In most transport measurements on normal metals, $\tau_{\text{s.o.}}$ is not an accessible quantity. In contrast, with localization experiments one can rather easily infer the spin-orbit scattering times in metal films.

In certain superconducting measurements, $\tau_{\text{s.o.}}$ can also be extracted. Using the data from superconducting tunneling and critical-field experiments, and from normal-state studies, Meservey and Tedrow[45] presented results for $\tau_{\text{s.o.}}$ in various metals to test the Z dependence of the spin-orbit time. The tunneling experiments[45] used films of thickness ~50 Å. Studies of the parallel-field superconducting critical fields[45,46] also used such very thin films. Tedrow and Meservey concluded that the scattering of the electrons from film boundaries was the mechanism likely to be responsible for spin-orbit scattering in the experiments they surveyed. By comparing their data

for Al, and data from other studies on other materials, the Z^4 dependence was also approximately demonstrated. However, the quantitative issue whether $\tau_{s.o.}$ scales with τ as given by Eq. (17) could not be demonstrated unambiguously, as this would require studies on samples over a wider range of elastic scattering times. Also, if the elastic scattering is due to impurities, and not due to a film-vacuum boundary, then the value to use for Z in Eq. (17) is not certain. In our experiments, $\tau_{s.o.}$ and τ are determined largely by bulk impurity scattering. We discuss these issues further in Sec. IV.

III. EXPERIMENTAL TECHNIQUES

A. Sample fabrication

The two-dimensional films studied in this work ranged in width from 250 μm down to 10 μm. They are fabricated using conventional contact optical photolithography.[47] The photolithographic mask was designed to facilitate a four terminal measurement of the completed film. Typically, 120 film squares were used.

Fabrication of narrow metal wires can be accomplished with a variety of techniques. The main techniques are electron-beam lithography, x-ray lithography, and step-edge (edge-defined) methods. All these techniques are summarized in Ref. 47. The step-edge methods developed by Prober *et al.*[48] have been used widely in past 1D localization studies. We have used x-ray lithography[49] for the present studies to fabricate 1D and 2D samples with (nearly) the same film properties. This allows a comparison of results of the 1D and 2D studies, providing a strong check on self-consistency. Due to the limitation of one-to-one pattern transfer in contact x-ray lithography, the x-ray absorber mask, of ~ 0.1 μm dimensions, must be made by either electron-beam lithography or step-edge methods. When the current studies began, only step-edge methods were available at Yale for mask fabrication.

The procedures used in the mask and sample fabrication sequence are shown in Fig. 1. Mask making involves etching a vertical step in a 1-μm-thick polyimide film, which was spun on a cover-glass slide. The polyimide film is nearly transparent to the exposing x-rays. Oxygen reactive-ion etching is used to form the step. A gold film ~ 1000 Å thick is the x-ray absorber. This is deposited across the etched step at an angle, leaving a gap at the base of the step. The width of this gap corresponds to the width of the metal wire to be produced. The initial height of the step and the angle of deposition of the gold film determine the width of the gap formed. A broad clear region for a contact pad was formed on either side of the wire by using a metal mask during gold deposition. A Cr layer (not shown in Fig. 1) is used to ensure good adhesion of the Au film. The polyimide membrane is bonded to a Vespel (polyimide) ring and the glass substrate is removed in hydrofluoric acid.[49] The glass would block the x rays if it were not removed.

The x-ray source is a Vacuum Generator EG-2 electron gun, with a water-cooled copper target. Electrons of approximately 6 keV energy are focused onto the target in a diffusion pumped chamber, at a pressure of $\sim 10^{-7}$ Torr. The x-ray resist, poly-methylmethacrylate (PMMA), is spun onto silicon wafers and is exposed through the x-ray mask. Intimate contact between the mask and the silicon substrate is ensured by an electrostatic mask hold-down technique.[49]

The use of resist lift-off in the fabrication of samples requires a directional deposition technique, such as thermal evaporation. To produce a small evaporation source, a wire of aluminum[50] is wound around a tungsten filament.[51] This is heated in a background pressure of $\sim 10^{-6}$ Torr in a standard diffusion pumped vacuum system. The film thickness is measured with a calibrated quartz-crystal monitor. The evaporation rates ranged from 2 to 20 Å/sec, depending on the film resistivity required. Cleaner films required larger rates. In the case of the narrow wires, we simultaneously codeposited wide films for comparison of film properties. In producing narrow wires, we oriented the tungsten evaporation filament parallel to the wire length (thus providing an effectively smaller evaporation source) to achieve improved lift-off.

B. Measurement techniques

The handling of samples after fabrication requires considerable care. This is especially true for the wires of width < 1 μm. In all cases we have found it useful to electrically short the leads on the substrate with silver paint before soldering external copper leads onto them. Pure indium solder was used for soldering these leads. After mounting the sample in the cryostat, an external shorting plug was used to keep the leads of the sample shorted; the silver paint shorting connections on the substrate were then scratched out. In addition, extra precautions, such as the use of a humidifier, were taken to avoid electrostatic buildup[52] during sample mounting. Some samples were "blown out" when such precautions were not followed.

During the experiments we had provisions for making (i) four-terminal resistance measurements using a dc current source and a nanovoltmeter[53]; (ii) four-terminal ac measurements of the resistance using a PAR-126 lock-in amplifier; and (iii) three-terminal resistance measurements using a LR-110 ac resistance bridge.[54] In a three-terminal bridge, the lead resistances are canceled if they are matched. While the four-terminal measurements were preferable for avoiding complications from contact resistances, they did not have the necessary resolution or stability. For the dc measurements, amplifier drift and noise were the limitations. For the four-terminal ac measurements, the stability of the ac current source and the amplifier and detector were the major limitations. For the low-resistance 2D samples ($R < 100$ Ω), we achieved the best resolution and sensitivity using the three-terminal ac bridge with the lock-in amplifier (with a 1:100 transformer input) as a detector. We could obtain a resolution and stability of better than 1 ppm as required for magnetoresistance studies on low-resistance samples even at relatively high temperatures. The noise observed was primarily the Johnson noise of the room-temperature balancing resistor of the bridge. For this three-terminal bridge,

the symmetric design of the leads in the mask for the two-dimensional samples made it possible to obtain a value for the sample resistance which was within 5% of the value found in the four-terminal measurements. For the high-resistance narrow wires, the LR-110 bridge with its own internal detector was adequate. The contact resistances (<1 Ω) were negligible compared to the wire resistance (>1 kΩ). In all the three-terminal measurements, for $T<3.5$ K we observed abrupt, but reproducible changes in the magnetoresistance due to the superconductivity of the indium contacts, which had $T_c \sim 3.7$ K. Four-terminal measurement could be used to eliminate this complication at lower temperatures. A frequency of 500 Hz was used for all ac measurements.

The cryostat used was designed originally by Dalrymple.[55] Temperature measurement was done using a calibrated germanium resistance thermometer. For temperatures above 4.5 K the sample was in an evacuated vacuum can; for temperatures below 4.5 K a small amount of He transfer gas was introduced. Temperature stability was ~ 1 mK. The temperature could be cycled using a heater imbedded in the same copper block as the sample and the thermometer.

The magnetic field required in the experiment was produced by a NbTi superconducting magnet described elsewhere.[55] We swept the magnetic field continuously, and recorded the resistance change with a chart recorder. Due to the relatively small characteristic fields H_i (~ 0.5 to 100 G) in our films, we did not need fields larger than 2 kG to observe the localization effects. Data for both positive and negative field sweeps were recorded to locate the true zero of the field. Different mounting stubs were used for parallel and perpendicular field measurements. The data were digitized manually, and then analyzed by a computer.

IV. EXPERIMENTAL RESULTS

A. Results for thin films

The films studied were 150—800 Å thick. $R_\square$ ranged from 0.17 to 6 Ω. The diffusion constant D, was determined directly from the superconducting critical field slope,[56] dH_{c2}/dT. The elastic mean free paths l were inferred for various samples assuming[57] $v_F = 1.3\times 10^8$ cm/sec. The $\rho_0 l$ products thus inferred indicated a tendency[12,58] to increase with increasing residual resistivity ρ_0, from a value of $\sim 2.5\times 10^{-12}$ Ω cm^2 for the cleanest films to a value of $\sim 5\times 10^{-12}$ Ω cm^2 for our highest resistivity films. The dirtier films had higher values of T_c, as is well known in the case of Al. The important sample parameters are given in Table I.

1. Perpendicular magnetoresistance

The details of the data fitting procedures are described in Ref. 8. The theoretical expression used included the contributions from localization and MT fluctuations [Eqs. (3) and (4)] and the fitting was done at low fields (<500 G). H_i and $H_{s.o.}$ were the fitting parameters. As discussed in Ref. 8, the polynomial form

$$\tau_i^{-1} = A_1 T + A_3 T^3 , \tag{18}$$

provides an excellent fit to the experimentally determined inelastic rate for a given sample. This suggests that two scattering mechanisms are operative in our films. We show in Fig. 2, our attempts to fit to functions of the form

$$\tau_i^{-1} = A_m T^m + A_n T^n ,$$

with $m=1$ and $n=2$, 3, and 4. Equation (18) is seen to correctly characterize the data. Other polynomial forms

TABLE I. Parameters for 2D films. $R_\square$ is at 4.5 K.

Sample	$R_\square$ (Ω)	d (Å)	T_c (K)	l (Å)	$\frac{A_1{}^a}{A_1^{\text{theor}}}$	$\frac{A_3{}^b}{A_3^{\text{theor}}}$
1	0.17	780	1.27	258	c	1.7
2	0.85	250	1.34	107	2.2	1.3
3	1.86	250	1.44	62	1.9	1.7
3a[d]	1.83	250	1.42	67	2.2[e]	1.9[e]
4	1.87	150	1.40	80	f	2.0
5	3.95	150	1.46	59	2.1	1.6
6	5.65	150	1.51	60	1.9	2.3
7	1.39	250	1.37	105	2.1	2.0
BR-A[g]	8.15	95	1.82	52[h]	1.9	1.5
BR-B[i]	33.0	90	1.83	23[h]	1.4	3.0

[a] A_1^{theor} is defined in Eq. (15).
[b] A_3^{theor} is defined by Eq. (13).
[c] This sample shows excess scattering at $T\sim 2$K; see text.
[d] 3 and 3a were deposited at the same time.
[e] Coefficients from perpendicular field MR analysis.
[f] At low temperatures this 10-μm strip shows precursors of a dimensional crossover effect. This precludes an accurate determination of A_1.
[g] Sample A of Ref. 66.
[h] The mean free path estimated from the $\rho_0 l$ product in our samples (Ref. 12).
[i] Also of authors of Ref. 66 (private communication).

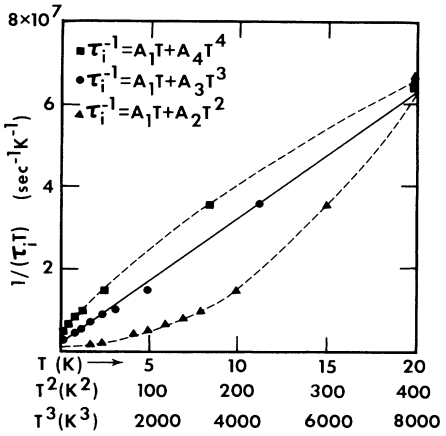

FIG. 2. Demonstration of the inadequacy of the various other polynomial forms for τ_i^{-1}. Inferred values of $(\tau_i T)^{-1}$ for sample 3 plotted vs T(▲); vs T^2 (●); and vs T^3 (■). The plots are artificially made to pass through the $T=20$-K point. The function that fits the straight line is the best fit. The straight line corresponds to $\tau_i^{-1}=A_1T+A_3T^3$. The dashed lines are guides to the eye.

for τ_i^{-1} with $m=2$ and $n=3$ and 4 did not give satisfactory fits either.

We now compare the coefficients A_1 and A_3 for the inelastic rate, Eq. (18), to the theoretical predictions outlined in Sec. II. The term linearly dependent on temperature corresponds to electron-electron scattering [Eq. (15)]. In Table I we show the magnitudes of the coefficients from both theory and experiment. They agree to within a factor of 2. Thus we find

$$\tau_i^{-1}=\tau_\epsilon^{-1}+\tau_{e\text{-ph}}^{-1}\ . \tag{19}$$

The inelastic mechanisms in our aluminum films are three-dimensional, clean-limit electron-phonon scattering and two-dimensional, dirty-limit electron-electron scattering.

2. *Comparison of inelastic rates to superconducting experiments*

An important outcome of our experiments is the quantitative understanding of the inelastic scattering mechanisms in our Al films. This helps us understand some "anomalous" behavior observed in superconducting tunneling experiments on Al films by Chi and Clarke.[59] They inferred an inelastic scattering rate (from the charge-imbalance relaxation rate in the superconducting state) which was larger than the electron-phonon inelastic rate. The measured rate increased with $R_\square$, though this correlation was not noted at that time.[60] We refer the reader to Ref. 8 for our detailed explanation of the experimental observation of Chi and Clarke. We found a satisfactory quantitative agreement between the inelastic scattering rate inferred from the superconducting experiments and our estimates for those samples with $R_\square > 1\ \Omega$ based on our localization experiments. Similar observation was also valid for the Al samples of van Son *et al.*[61,8] in their microwave superconducting gap enhancement experiments. This agreement on inelastic scattering rates (of samples of comparable sheet resistance) between the localization and superconductivity experiments poses an important theoretical question. The inelastic scattering that enters the theories relevant to the various superconductivity experiments[62] may, in principle, differ from the inelastic scattering in localization experiments that causes the relaxation of the localization phase coherence. However, Fig. 3 of Ref. 8 indicates that these two mechanisms have comparable magnitudes in Al films. Such an observation could be interpreted as due to the strongly inelastic nature of the electron-electron and electron-phonon scattering processes. If the electron scattering processes were quasielastic, the phase relaxation rate and the inelastic rate should be very different.[37,38]

In the low resistance ($R_\square < 1\ \Omega$) films of Chi and Clarke, and also those of van Son *et al.*, electron-phonon and dirty-limit electron-electron scattering rate are too small to account for the experimental rates. We speculate[8] that in these cleaner films the relevant electron-electron scattering mechanism should correspond to the clean limit ($\hbar/\tau < k_B T$). The calculations of MacDonald[32(b)] for the phonon-enhanced electron-electron scattering in bulk Al yields a value that agrees also with a factor of ~ 3 with the excess scattering observed in our clean sample. Our data for sample 1 are also consistent with such a term, but the data are only reliable from 2–6 K, due to the small size of the fractional resistance change. As a result, this issue cannot be resolved at present. Clean-limit 2D electron-electron scattering[36] has been found to play a role in MOSFET's.[63] More theoretical and experimental work is needed on metal films in this regime of low $R_\square$.

3. *Resistance as a function of temperature*

Most of the early localization experiments used thin films of nonsuperconducting metals, and observed a resistance increase with decreasing temperature. However, since our sample material is aluminum, the resistance decreases as T is reduced at the lowest temperatures due to the superconducting fluctuations. The experimental data for $\tilde{\delta}R(T)/R$ for sample 7 in the temperature range 2 to 16 K are shown in Fig. 3. The theory fits include the contributions from classical electron-phonon scattering, localization and MT fluctuations. The contribution to the $R(T)$ due to electron-electron scattering[24] is negligible compared to the other contributions. The data are shown for zero field and at $H=20$ G. We find the phonon contribution is well fit by $\tilde{\delta}R^{\text{ph}}/R = C_{\text{ph}}T^3$. There are three fitting parameters, H_i, $H_{\text{s.o.}}$, and C_{ph}, needed to predict $R(T)$. Of these, H_i and $H_{\text{s.o.}}$ were determined from the magnetoresistance fits, and are *not* adjustable here. Only C_{ph} was taken as a "free" parameter.

In Fig. 4 we show the $R(T)$ for sample 7 in zero applied magnetic field decomposed into individual contributions. The general shape of the $R(T)$ curve is due to the fact that at high temperatures the electron-phonon scattering contribution (as discussed in Sec. II D) is dom-

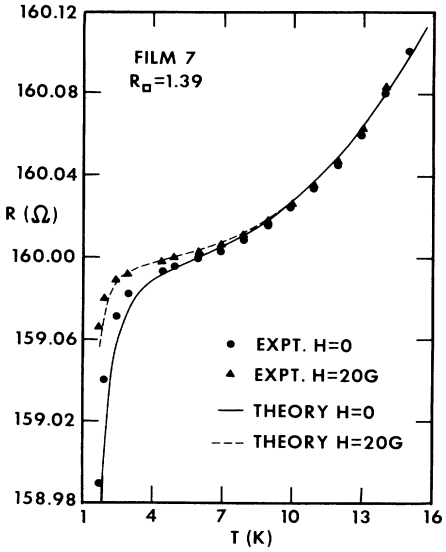

FIG. 3. Resistance vs temperature for 2D film sample 7. The theory fit was matched to the experimental data at $T=6$ K. The only fitting parameter was $C_{\rm ph}=1.9\times10^{-7}$.

inant. At the lowest temperatures, the Maki-Thompson term [Eq. (5)] is dominant. Hence, from the studies of $R(T)$ alone an unambiguous extraction of the localization contribution would not be possible. However, in our fitting of the magnetoresistance we found that $H_{\rm s.o.}\ll H_i$ at high temperatures and $H_{\rm s.o.}\gg H_i$ at low temperatures. An estimate of the *localization* contribution reveals that as the temperature *decreases* from 20 to $\sim$8 K, the fractional resistance increase is only $\sim2\times10^{-5}$. This magnitude is *only about a tenth* of the value predicted by the localization theory if one ignores spin-orbit scattering. Below $\sim$8 K, Eq. (3) and the inferred values of τ_i and $\tau_{\rm s.o.}$ predict

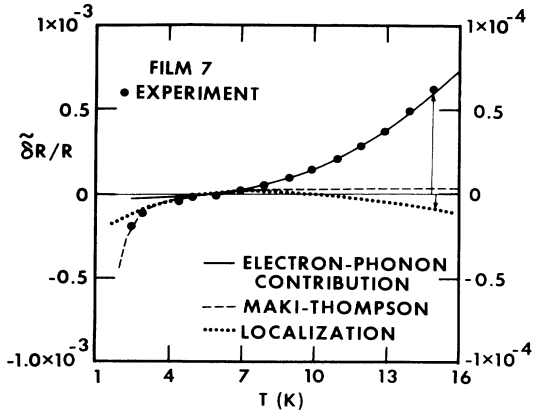

FIG. 4. Decomposition of $R(T)$ for sample 7 into individual components. For the localization contribution only (dotted line), the enlarged vertical scale on the right applies. For $T>7$ K, the electron-phonon term is dominant and for $T<4$ K, the MT term is dominant. For 4 K $<T<7$ K, all the terms are comparable and small. Reference temperature is 6 K.

that the localization resistance *actually decreases* with further *decrease* in temperature. The MT contribution, in contrast, can be unambiguously identified since it diverges as $T\rightarrow T_c$. The inferred inelastic rate from the magnetoresistance studies is also consistent with the observed MT contribution to $R(T)$.

The value of $C_{\rm ph}$ derived in the above analysis for each sample, should be related to the value of A_3 inferred from our analysis of the magnetoresistance data. Using a simple Drude model,[18] we predict that

$$\rho_{\rm ph}/\rho_0=A_3T^3/\tau^{-1}=[(A_3l)/v_F]T^3\ ,$$

so that we should find $C_{\rm ph}=A_3l/v_F$. This formula for $\rho_{\rm ph}$ applies if *all inelastic scattering* events contribute to the resistance and there is no restriction to small scattering angles. The absence of a restriction on scattering angles is due to the fact that umklapp scattering is significant in Al even at very low temperatures.[24,64] We find $C_{\rm ph}=A_3l/v_F$ to within a factor of 2. We conclude that sensible electron-phonon inelastic rates explain both the magnetoresistance and the $R(T)$ data. This strengthens further our identification of this inelastic mechanism.

4. *Parallel-field magnetoresistance*

The goal of the parallel-field studies was to verify the theoretical prediction for parallel fields and see if the parameters H_i and $H_{\rm s.o.}$ inferred from an analysis of the parallel-field data are the same as those for perpendicular fields. For one film sample, 3a, we have done measurements in both the parallel and the perpendicular field orientations. 3a was deposited at the same time as 3 but was measured about a year after 3 was measured.

First, perpendicular field measurements on 3a were done as described previously. All the sample parameters were in good agreement with those of 3 for both the basic film properties (see Table I) and also for the inferred values of $\tau_{\rm s.o.}$ and τ_i. The sample was next mounted on a stub designed for parallel fields and measured on a different day. We did *not* attempt to verify the deviation from the parallel orientation in a systematic fashion, and hence cannot rule out the possibility that there was a small perpendicular component of the field. However, in order to avoid a more complicated analysis with an additional unknown parameter (tilt angle), we have chosen to do the analysis using only the parallel field theory, and look for consistency in the values of the inferred parameters.

The qualitative behavior for the parallel and perpendicular field data is similar. Figure 5 shows the data for sample 3a at 4.5 K in parallel and perpendicular fields. At these low temperatures, the sample showed positive magnetoresistance in perpendicular as well as parallel field. Negative magnetoresistance was observed at high temperatures for both the parallel and perpendicular configurations. This confirms right away that the relative magnitudes of H_i and $H_{\rm s.o.}$ were the same for the two field orientations, as indeed they should be. However, there is appreciable magnetoresistance at low fields in the perpendicular orientation. In the parallel orientation one needs a field typically $\sim$30 times larger for a comparable

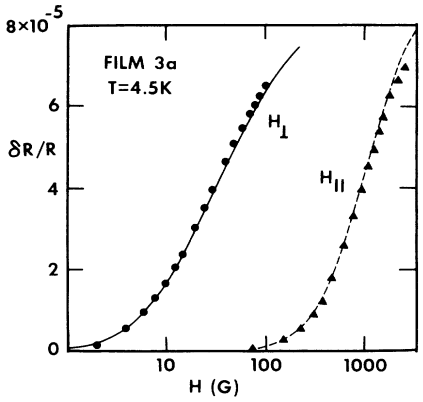

FIG. 5. Comparison of parallel and perpendicular magnetoresistance data for sample 3a. The fit parameters are $H_i = 1.35$ G and $H_{s.o.} = 21$ G for the perpendicular field data (●). For the parallel field data, the fit parameters are $H_i = 1.8$ G and $H_{s.o.} = 31.5$ G.

size magnetoresistance.

The theory used in fitting the experimental data includes the localization and MT terms as described in Sec. II. As indicated there, the theory for parallel fields is a perturbation calculation and valid only for fields $H < 12H_d$. Since $d = 250$ Å, this condition restricts the applied fields to less than ~ 10 kG. Our measurements were only up to ~ 2 kG. We use the same value for the parameter β (taken from Larkin's calculation[7(a)]) for both orientations. The inferred values of H_i and $H_{s.o.}$ are different by a factor of 1.5 for the two different field orientations. We consider this to be satisfactory. Fits of a quality similar to that of Fig. 4 are obtained for all temperatures below ~ 10 K for the parallel field data.

At temperatures above 10 K there is a measurable MR ($\delta R/R > 10^{-7}$) only at higher fields, > 1 kG. In this case, other contributions, such as classical magnetoresistance, cannot be ignored. For this temperature and field region, to obtain a satisfactory fit for the MR data we include a third term in the theory in addition to localization and MT terms. This term is proportional to H^2. The coefficient of this term is not a strong function of temperature. We interpret the third term as due to classical MR and this contribution is likely isotropic if $l < d$. We can obtain an estimate of the classical magnetoresistance from our perpendicular field measurements on three cleaner samples at higher fields. These measurements indicate that

$$\delta R^{\rm cl}/R = 0.9(lH)^2 ,$$

where l is in cm and H is in G. We find that the term which is required to explain the experimentally observed *parallel*-field magnetoresistance corresponds fairly well to this classical magnetoresistance term. We note that while the theoretical prediction for the electron-electron interaction term is also proportional to H^2, the predicted effect is a function of temperature. It is also smaller than the experimentally observed H^2 term by at least one order of magnitude, in any case.

Thus, the experiments on parallel magnetic fields show good agreement with the theory for the localization and MT contributions. The film parameters and scattering rates are in reasonable agreement with the perpendicular-field results.

5. *Spin-orbit scattering*

We plot in Fig. 6 the values of $\tau_{s.o.}$ inferred from our magnetoresistance data. The plot is done as a function of τ for the eight samples. l was obtained from H_{c2} measurements, using $v_F = 1.3\times 10^8$ cm/sec. We also show the results from previous nonlocalization experiments for comparison. The solid line corresponds to $\tau/\tau_{s.o.} = 2\times 10^{-4}$. The approximate proportionality[65] of τ and $\tau_{s.o.}$ seen for our data in Fig. 5 allows one to argue that spin-orbit scattering arises from the same events that cause elastic scattering. Of course, spin-orbit scattering is much less probable. Equation (17) predicts $\tau/\tau_{s.o.} = 0.8\times 10^{-4}$ if one uses $Z = 13$ for Al. As noted before, the choice of the appropriate ion charge Z to use in Eq. (17) is an issue which is not fully resolved. If the scattering were caused by vacancies, lattice defects, or were due to a metal/vacuum interface, Z should be the nuclear charge of Al, 13. If the dominant scattering mechanism were scattering from impurities, the appropriate value for Z may be that of the impurity.

In our samples, the elastic mean free path, as inferred from the critical field measurements, is smaller than the film thickness. Thus, τ is determined by scattering within the film. The elastic mean free path decreases when the films are deposited at a slower rate in the vacuum chamber. The incorporation of residual oxygen into Al films from the deposition chamber has been thought to be the reason for this observed behavior. However, the use of $Z = 8$ (corresponding to oxygen) gives a predicted magnitude for $\tau/\tau_{s.o.}$ that is 20 times smaller than the experi-

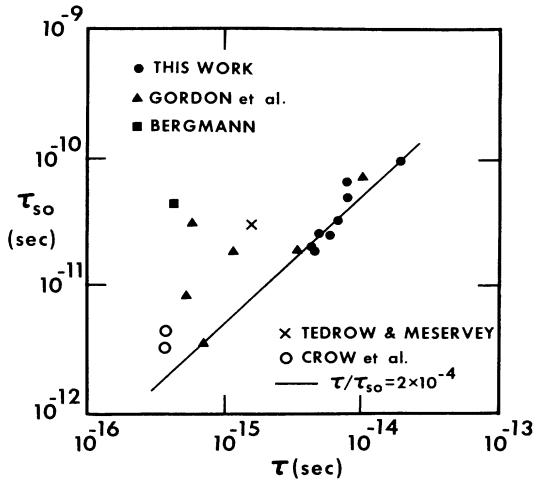

FIG. 6. Spin-orbit time in Al as a function of the elastic scattering time. The results from nonlocalization experiments (Refs. 45 and 46) and localization experiments (Refs. 13, 58, and 60).

mentally observed value. Thus, a quantitative understanding of the spin-orbit scattering rate remains elusive. We should, nevertheless, point out that the spin-orbit rate generally increases with increasing atomic number as demonstrated by other experiments, particularly those of Bergmann.[3] We discuss the results of the other localization experiments on thin films of Al in Sec. V.

Prior to localization experiments, Meservey and Tedrow[45] had obtained spin-orbit scattering rates in Al films from an analysis of tunneling data. Crow *et al.* studied upper critical magnetic fields in thin Al films to obtain $\tau_{s.o.}$. We show the results from these superconducting experiments also in Fig. 6 for comparison. These experiments yield a value for $\tau/\tau_{s.o.} \sim 3$ times smaller than our value.

B. Results for narrow wires

The wires we have studied had thicknesses of either 150 or 250 Å. The properties of these wires are given in Table II. The wires were observed in a scanning electron microscope after the low-temperature experiments to determine their width. The wire length was $\sim 210\ \mu$m. The value of $R_\square$ was experimentally inferred, using the measured width and length and sample resistance. This value of $R_\square$ was smaller than that of the codeposited wide film by $\sim 20\%$ in the best case, and by $\sim 50\%$ in the worst case. A variety of effects in the deposition process (e.g., for the narrow wires, reflection of Al atoms off the resist wall) might cause this difference in $R_\square$. In our analysis we have used the experimentally determined values of $R_\square$. The width of a given wire was uniform to $\sim 5\%$.

The two-dimensional films showed the expected linear behavior for H_{c2} close to T_c, $H_{c2} \propto T_c - T$. In contrast, the narrow wires showed

$$H_{c2} \propto (T_c - T)^{1/2}, \tag{20}$$

for fields perpendicular to the plane of the wire. This corresponds to the case where the temperature-dependent superconducting coherence length $\xi(T)$ is larger than the sample width. This situation, then, is similar to a superconducting thin film in parallel field[56] where the dependence of H_{c2} on $T_c - T$ is also given by Eq. (20).

1. *Fully one-dimensional samples*

Most of the results on one-dimensional Al wires were previously reported in Ref. 10. To be in the fully-one-dimensional regime we require samples of width $W < l_i$ *and* $l_{s.o.}$. The theoretical expression for the magnetoresistance fits included the localization and MT contributions, given by Eqs. (8) and (9). Since the theoretical result was a perturbation calculation[9] for small fields, the fitting was done only up to 300 G. For sample A, the field limit for Eqs. (8) and (9) is ~ 350 G.

From our fits we find that the magnetoresistance of samples A and B obeys the one-dimensional form over the entire temperature range 1.8 to 15 K. Fits to the two-dimensional theoretical form were not satisfactory. The inelastic scattering length $l_i(T)$ inferred from these fits for sample A is reproduced from Ref. 10 as Fig. 7. For comparison, we show $l_i(T)$ for the co-deposited wide (2D) film. The agreement seen in Fig. 7 is excellent. Similar agreement is seen for the other fully-1D wire, sample B.

The agreement of the inelastic scattering rates in Fig. 7 was the first reported agreement of inelastic rates for samples of different localization dimensionality. Before we try to understand this result we note that the mechanisms that contribute to the inelastic processes in 2D films are electron-phonon scattering and electron-electron scattering. As discussed in Sec. II D above, the dimensional size scale for electron-phonon scattering is the characteristic phonon wavelength. At the temperatures where the electron-phonon scattering is dominant, typically $T > 5$ K, both the films and the narrow wires are three-dimensional with respect to electron-phonon scattering. The films and wires should have the same effective dimensionality since $\lambda_{ph} < W$. Hence, the magnitude of the electron-phonon scattering rate is expected to be the same in both our films and wires. At low temperatures, electron-electron scattering begins to dominate. The dimensionality for the electron-electron scattering is decided by a different characteristic length scale from that of electron-phonon scattering. We initially thought Eq. (14) to be the relevant theoretical result for electron-electron scattering, with a typical energy of $\sim k_B T$. Hence we proposed in our previous publications[9–11] that the wires were two-dimensional also with respect to the electron-electron inelastic mechanism, since $W > (\hbar D/k_B T)^{1/2}$. More recently (as discussed in Sec. II D) electron-electron scattering at small energy transfers has been understood to contribute significantly to the phase relaxation. The correct theoretical prediction should be Eq. (16) for one-dimensional systems, such as we have studied. The condition Eq. (16a) for the use of the 1D electron-electron scattering rate for the material properties of the wire A is

$$W < (6/T^{1/2})$$

with W expressed in μm and T in K. Since sample A is only 0.2 μm wide, it easily satisfies the condition for one

TABLE II. Parameters for narrow wires. $R_\square$ is at 4.5 K.

Sample	$R_\square$ (Ω)	d (Å)	T_c (K)	W (μm)	$l_{s.o.}$ (μm)	l_i (4.5 K) (μm)
A	0.9	250	1.35	0.20	0.48	1.47
B	1.2	240	1.34	0.24	0.57	1.28
C	2.8	150	1.45	0.60	0.32	0.98
D	4.5	150	1.49	0.40	0.30	0.78

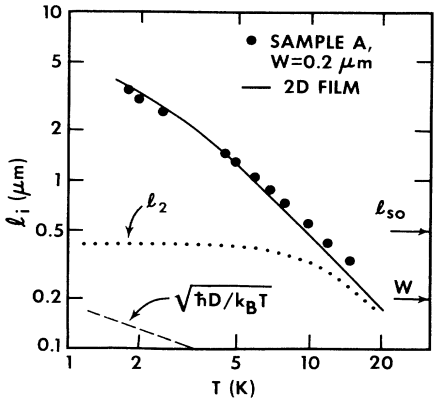

FIG. 7. Inelastic diffusion length vs temperature. The solid line is the experimentally determined l_i for the codeposited wide film. Up to 15 K, $W < l_2$ and l_i as required for fully one-dimensional behavior. $l_{s.o.}$ is the spin-orbit scattering length $(D\tau_{s.o.})^{1/2}$.

dimensionality. For sample A, a comparison of the magnitudes of the τ_ϵ^{-1} at $T=4$ K for the 2D and 1D cases [Eqs. (15) and (16), respectively] reveals that the 1D rate is larger than the 2D rate by a factor of ~ 5. This difference in the inelastic scattering rate is expected to result in a value of l_i that is ~ 2 smaller than for the film. Hence, we *should have observed* the one-dimensional electron-electron scattering mechanism. We apparently *did not.* Due to the dominance of the electron-phonon scattering at higher temperatures we have only a limited temperature range (1.8 K $< T <$ 5 K) to observe the change in the dimensionality of electron-electron scattering. In any case, the agreement of electron-phonon scattering rates at higher temperatures for the wires and the films unambiguously confirms the one-dimensional behavior with respect to localization. We also note that the qualitative validity of Eq. (16) has not been verified yet by experiments.

Most previous studies of narrow wires measured in detail only the resistance change with temperature. For our samples, magnetoresistance data and the resulting τ_i values provide the most direct test of localization theory. As shown in Ref. 10, the theoretical predictions based on contributions from localization, MT fluctuations and classical electron-phonon scattering *quantitatively* explain the experimental data. The electron-phonon part of $R(T)$ is indeed well fit by $\tilde{\delta}R^{\rm ph}/R = C_{\rm ph}T^3$ for the wires, independent of H. This is just the same as in the case of thin films discussed previously. The values of $C_{\rm ph}$ for the 2D and 1D cases agree within 5%. The quantitative agreement of theory and experiment over the entire temperature range of Fig. 3 of Ref. 10 confirms the 1D theoretical prediction. At low temperatures the MT term is dominant. The fact that at low temperatures it is the 1D theory which correctly describes the experimental data confirms that l_i is the relevant length scale for the MT term.

2. *Mixed-dimensional samples*

When the sample width is such that $l_2 < W < l_i$, we expect to observe mixed-dimensional behavior, as noted in Sec. II B. We have studied two samples, C and D, which are in this regime. We illustrate the case using sample C, of width 0.6 μm.

The magnetoresistance data for sample C can be satisfactorily fit to the 2D theory at high temperatures, 15 and 20 K. At 15 K, $l_i = 0.25$ μm. $H_{s.o.} = 16$ G, independent of temperature, which implies $l_{s.o.} \sim 0.3$ μm. Thus, the behavior of this wire should indeed be two dimensional at high temperatures. In contrast, for $T < 12$ K, the experimental data cannot be fit satisfactorily to the 2D magnetoresistance theory for any set of parameters H_i and $H_{s.o.}$. However, when $T < 6$ K the behavior of the sample is well described by the magnetoresistance formula corresponding to mixed-dimensional behavior, namely, a 1D singlet localization term and a 2D triplet term. The same value of $l_{s.o.}$ is obtained here as at the higher temperatures. At these lower temperatures, the fully-1D theory does not provide as good a fit as the mixed-dimensional theory. (At the very lowest temperatures, $T \sim 2$ K, the MT contribution and the singlet localization contribution are completely dominant, so that at 2 K it is hard to distinguish the mixed-dimensional result from the fully-1D result. Studies of nonsuperconducting wires would remove this ambiguity.) The inferred inelastic scattering length for sample C is plotted as a function of temperature in Fig. 8 along with those for the codeposited wide 2D film. The agreement of the inelastic rates corroborates the predictions of the mixed-dimensional theory.

Experimentally, when $l_i > 1.3W$, the mixed-dimensional theory is found to be applicable. When $l_i < 0.5W$, the 2D theory is applicable. Thus, for the singlet and MT terms there is indeed a crossover in dimensionality when $l_i \sim W$.

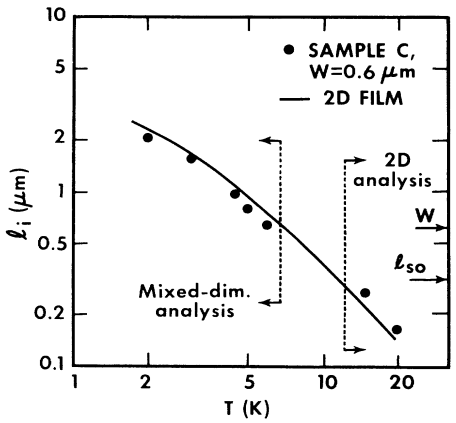

FIG. 8. Inelastic diffusion length vs temperature for a wire of intermediate width; at low temperature ($T \leq 6$ K), the localization behavior is of mixed dimensionality, as $l_2 < W < l_i$. For $T \geq 15$ K, the localization behavior is that of a 2D film, since $(l_2, l_i) < W$. In each temperature range appropriate theoretical analysis was used to extract values of l_i.

This crossover of localization dimensionality is in accord with the original ideas of Thouless.[1]

V. COMPARISON TO OTHER WORK

A. Other studies on Al

Due to the vast number of studies on two-dimensional and three-dimensional systems we shall not give a full account of these other results in this article. Numerous studies have confirmed the predictions of the 2D localization theory. Very elegant studies by Bergmann[3] have even demonstrated directly the important role of spin-orbit scattering. However, a consistent understanding of the phase-breaking time τ_i in metal films had not emerged from previous studies. A number of studies showed an inelastic rate $\tau_i^{-1} \propto T^p$, with $p \sim 2$ in many experiments.[3] The magnitude of this T^2 rate is generally too large to be explained by known mechanisms. Not all experiments show this dependence. Furthermore, not all experiments on (nominally) the same material have the same results for τ_i^{-1}. We refer to the recent review by Bergmann[3] for a thorough account of these conclusions.

There are fewer experiments on superconductors (at $T > T_c$) than on normal metals ($T_c = 0$). Many of the studies on superconductors have been on aluminum, since a relatively low but accessible T_c is required to allow measurements over an extended temperature range. While it is not evident in the published literature, there is rather good consistency among all these studies on Al films, both for the experimental data and for the inferred scattering times, if a consistent scheme of data analysis is employed. We will discuss these other experiments on aluminum samples in detail here.

Bruynseraede *et al.*[66] studied Al films of $R_\square$ ranging from ~ 1.5 to 60 Ω. These films were approximately 100 Å thick. For their analysis they used the localization theory in the limit of no spin-orbit scattering. Their inferred inelastic rates showed an approximately linear dependence on T but were larger than the predictions of the electron-electron scattering theory [Eq. (14)] by one order of magnitude. We have reanalyzed[8] their magnetoresistance data for their sample A in the manner described in this work (i.e., without assuming $\tau_{s.o.}^{-1} = 0$). The results for τ_i^{-1} which we then obtain for their sample are *consistent* with the rates in our own samples. The inelastic rates for their samples are thus consistent with the theory, Eqs. (18) and (19). Bruynseraede and colleagues[66] now agree with our method of analysis and the conclusions on their data stated here. The analysis presented in their original work was merely too simplified.

The work of Gordon *et al.*[58,60] is an interesting complement to the work reported in this paper. They initially studied granular, high-resistivity films, with $l \sim 15$ Å. They fit their 2D magnetoresistance data to the complete theoretical form, and found the inelastic rate to be given by Eq. (19) *as was found in this work*. In their original analysis they had found[60] that the electron-phonon mechanism showed $\tau_{e\text{-ph}}^{-1} = A_4 T^4$ for films with $l < 15$ Å and $\tau_{e\text{-ph}}^{-1} = A_3 T^3$ for a film with $l = 46$ Å. They have recently studied cleaner films and also reanalyzed their original data.[58] Gordon *et al.* have concluded that the form $\tau_{e\text{-ph}}^{-1} = A_3 T^3$ describes the experimental data well for all of their samples. Their experiments spanned a wide range of $R_\square$ (~ 2 to ~ 200 Ω) and thickness ($d \sim 70$ to 200 Å). The coefficient A_3 appeared to increase from our value of $\sim 1.5 \times 10^7$ to $\sim 3.5 \times 10^7$ with increasing resistivity. Their earlier identification of an electron-phonon scattering rate proportional to T^4 was due to the relatively small contribution of electron-phonon scattering in the high-resistance films. It was difficult to distinguish between a T^3 and a T^4 dependence for those data. The contrasting case for low $R_\square$ films is shown in Fig. 2 above.

Gershenson *et al.*[67] reported measurements on two aluminum films with $R_\square = 20$ and 112 Ω. The films were ~ 50 Å thick. They analyzed their MR data assuming the samples were in strong spin-orbit scattering limit at low temperatures, and in the zero spin-orbit scattering limit at high temperatures. They found that the low-resistance film showed $\tau_i^{-1} \sim T^2$ behavior in the entire temperature range. The high-resistance sample showed $\tau_i^{-1} \sim T$ at low temperatures and $\tau_i^{-1} \sim T^2$ at high temperatures. Gershenson *et al.* concluded that the T^2 dependence of the rate was due to *two-dimensional* electron-phonon scattering. We have reanalyzed their magnetoresistance data for the low-resistance sample without specific restrictions on the relative magnitudes of $\tau_{s.o.}$ and τ_i. We find that the data could indeed be fit well using the method described in this article (with a temperature-independent value for $\tau_{s.o.}$). This reanalysis yielded inelastic rates which can also be interpreted[12] in terms of two-dimensional electron-electron scattering and *three-dimensional* electron-phonon scattering as in the case of our samples. The electron-electron coefficient A_1 is in good agreement with the theory of Alt'shuler *et al.*[37] as is found in our work. However, the electron-phonon coefficient A_3 for their data appears to be larger ($A_3 \sim 3 \times 10^7$) consistent with the observations of Gordon *et al.*[58] We should point out that it may be surprising that such a thin film ($d \sim 50$ Å) should behave as a three-dimensional system for electron-phonon scattering. The issue of the dimensionality of electron-phonon scattering in thin films definitely deserves further study.

A quench condensed Al film of $R_\square = 117$ Ω and thickness 90 Å was studied by Bergmann.[13] He fit the MR data to the complete theory including spin-orbit scattering. He inferred a behavior of $\tau_i^{-1} \propto T^{2.13}$ in the temperature range 4.5 to 20 K. Bergmann contended that quench condensed films were intrinsically different from pure Al or granular Al. In spite of all the differences in the preparation of the samples, the basic film properties (such as T_c, low-temperature resistivity and the diffusion constant) and even the inferred spin-orbit scattering rate are close to those of the granular film sample C of Gordon *et al.*[60] An evaluation of τ_i using the inferred coefficients A_1 and A_3 from the work of Gordon *et al.* can likely explain Bergmann's data in quantitative terms. It is also likely that if Bergmann had obtained the experimental data over a wider temperature range, any deviation of the data for τ_i^{-1} from a single power-law (T^n) behavior would have been more obvious. Indeed, τ_i at the lowest temperature studied, $T \sim 4.5$ K (see Fig. 10 of Ref. 13) deviates

from the value one would obtain from an extrapolation of the high-temperature data assuming $\tau_i^{-1} \sim T^{2.13}$!. This indicates a slower temperature dependence at low temperatures than $\tau_i^{-1} \sim T^{2.13}$, and is consistent with our findings and those of Gordon *et al.*

Shinozaki *et al.*[68] have recently reported the MR studies of a granular Al film with $R_\square \sim 315\ \Omega$ and thickness ~ 100 Å in the temperature regime 4.2 to 35 K. Using an analysis similar to ours for the MR data, they infer an inelastic rate proportional to T at low temperatures in agreement with our results. But at the higher temperatures they find the inelastic rate to be proportional to T^2. We note that this film had the highest $R_\square$ of all the Al films studied so far and hence the electron-electron scattering rate predicted by Eq. (15) is very large as a result. Figure 2 of Ref. 67 clearly shows the linear dependence of the inelastic rate [Eq. (15)] up to ~ 10 K. If we assume that the magnitude of the electron-phonon rate for this film is given by $\sim 3\times 10^7 T^3$ (as obtained by Gordon[58] in his high-resistivity films), then only for $T > 20$ K, does the electron-phonon contribution begin to be appreciable. Thus, for temperatures larger than $T \sim 20$ K one sees a deviation from the linear behavior expected from Eq. (15). Only above $T \sim 35$ K, does the magnitude of the electron-phonon scattering dominate. Hence the conclusion of Shinokazi *et al.* that the inelastic scattering rate is proportional to T^2 at high temperatures is likely to be an artifact of the limited temperature range studied. For such high resistance of the films, the electron-electron scattering rate is very large and a broader temperature range must be studied to correctly extract $\tau_{e\text{-ph}}$.

Magnetoresistance measurements on 1-μm-thick granular Al films with resistivities in the range ~ 300 to 6000 $\mu\Omega$ cm were reported by Mui *et al.*[69] The film morphology is that of Al grains ~ 30-Å diam, isolated from adjacent grains by aluminum oxide. The analysis was done in terms of the three-dimensional theory, comprising terms from localization, MT fluctuations and the orbital contribution of the electron-electron interaction. The inferred inelastic scattering rate appeared to change from $\tau_i^{-1} \propto T^2$ in the case of the ~ 300-$\mu\Omega$ cm sample to $\tau_i^{-1} \propto T$ for the ~ 6000-$\mu\Omega$ cm sample. The magnitude of the inelastic scattering rate appears to be comparable to the 2D case. These samples can be shown to be in the three-dimensional limit for the electron-electron scattering.[37,38] In this case, electron-electron scattering events with a characteristic energy transfer of $\sim k_B T$ are expected to dominate[16,37] resulting in $\tau_{e\text{-}e}^{-1} \propto T^{3/2}$ behavior.[29,35] It is likely that electron-phonon scattering in their low-resistivity samples is not negligible so that

$$\tau_i^{-1} = \tau_{e\text{-}e}^{-1} + \tau_{e\text{-ph}}^{-1} .$$

The nature of electron-phonon scattering in such granular systems is unknown. The samples with resistivity ~ 1000 $\mu\Omega$ cm may indeed have an inelastic mechanism corresponding to two-level tunneling states (TLS) with a rate[42] $\tau_{\text{TLS}}^{-1} \propto T$.

We wish to comment briefly on the values of $\tau_{s.o.}$ inferred in the other localization experiments on aluminum. The ratio for $\tau/\tau_{s.o.}$ for some of the films studied by Gordon *et al.*[58,60] *does agree* with the values we find. (See Fig. 6 above.) But Gordon *et al.* observed the ratio $\tau/\tau_{s.o.}$ to be smaller by as much as one order of magnitude in their other high-resistance films. No systematic behavior was obvious in their work. In general, Al films of higher resistivity are produced by evaporating in an oxygen atmosphere.[58,68] The conduction in these films occurs by the electron tunneling through the oxide barriers. For these granular films the ratio $\tau/\tau_{s.o.}$ (if τ is derived from the film resistivity) appears to be quite different in magnitude from our results. The work of Mui *et al.*[69] on three-dimensional localization in granular Al showed a value almost three orders of magnitude smaller for $\tau/\tau_{s.o.}$ than we find for our cleaner films. We suggest that this difference in behavior may be traceable to the different conduction mechanism in the granular case. Weak tunneling between grains determines the resistivity for the granular films, but apparently does not contribute to spin-orbit scattering. The mechanism(s) causing spin-orbit scattering in granular Al films must be different from that in our "pure" Al films. The quench condensed Al film of Bergmann[13] also showed a smaller value for the $\tau/\tau_{s.o.}$ ratio (see Fig. 6). However, it is interesting to note that Shinozaki *et al.*[67] find $\tau/\tau_{s.o.} \sim 10^{-4}$ in their granular film. Thus, a detailed understanding of the spin-orbit scattering mechanism in granular films will require further study.

B. One-dimensional studies

In a recent publication[11] we have presented, in detail, our conclusions of a reanalysis of the previous experimental studies on lithographically defined narrow wires of Au-Pd,[43(a)] Pt,[43(b)] W-Re,[70] and Cu,[71], drawn Pt wires,[72] and Bi whiskers.[73] We shall not repeat the details here, but rather will give a summary of our conclusions to provide an understanding of the complete picture for the one-dimensional systems studied to date.

For the alloys Au-Pd and W-Re, it appears that magnetic scattering and/or large spin-orbit scattering rates gave very small localization effects compared to interaction effects. The resistance changes with temperature measured in those early studies appear to have been due to electron-electron interaction effects! Even with this interpretation, it is still not understood why the fractional change of resistance at low T depended linearly on the resistivity of the sample (in the case of Au-Pd, W-Re, and Pt wires[41(b),74]). We refer to a recent article by Masden and Giordano[74] that summarizes their conclusions on this question for their experiments on Pt and Au-Pd. In the case of the Cu wires, the resistance rise is also likely due to interaction effects as was noted by the authors. The localization effects may have been absent due to magnetic scattering. There may also be a large phase relaxation rate due to new one-dimensional mechanisms. In the Bi whiskers the observed resistance decrease with decreasing temperature may have been due to "antilocalization" caused by the presence of strong spin-orbit scattering. In the drawn Pt wires the observed magnetoresistance was not due to 1D localization effects. The observed behavior was probably due to large disorder produced by the drawing process, as indicated by the authors.

We note that there have been recent studies by Gordon[75] on an Al wire, Licini *et al.*[76] on Li wires and by Lin and Giordano[77] on a Au-Pd wire. The magnetoresistance behavior observed by these three experimental groups fully confirms our conclusions on the success of the theory of weak localization in explaining the experimental data. Godfrin *et al.*[78] observed a 1D-to-2D crossover in the temperature dependence of resistance in Ga-As wires and determined the inelastic scattering lengths in those samples.

The studies discussed so far have all used metal or semiconductor[78] wires. It is also possible to form narrow inversion layers in silicon MOSFET's. Studies of such quasi-1D MOSFET's in the weak localization regime ($\delta R/R \ll 1$) have been carried out by Wheeler *et al.*[79] and by Skoçpol *et al.*[80] We discuss here the work by Wheeler *et al.*, as it is more quantitative in its analysis. The results of Skoçpol *et al.* appear to be consistent with those of Wheeler *et al.*

Wheeler *et al.*[79] studied narrow metallic wires formed in silicon inversion layers of width ~ 0.3 μm. The MR studies showed clearly the presence of localization in these systems. In a prior analysis of data for wide (2D) MOSFET's, Wheeler *et al.* had identified the dominant inelastic mechanism there to be dirty-limit 2D electron-electron scattering. The inelastic electron scattering mechanism in the narrow wires appeared to be 1D dirty-limit electron-electron scattering for the 1D (narrow) wire. This result is to be contrasted with our data in Fig. 7, which shows only a change in the localization dimensionality but not in the inelastic rate. Also, Eq. (16) for the electron-electron scattering rate in 1D systems gives an estimate of τ_ϵ for the narrow MOSFET sample that is larger than the value experimentally inferred by Wheeler *et al.* For our work, Eq. (16) predicts a value for the inelastic scattering time in the wires that is smaller than what we find experimentally. We do now know the reason for these discrepancies. One possible source of this difference is that the theoretical equation for δR used in Eq. (3) of Ref. 79 had an additional factor of 2 in the denominator compared to the expression we obtain, Eq. (8) with $H_{s.o.}=0$. This raises some difficulties in the quantitative understanding of the results of Wheeler *et al.* in light of our experiments. In any case, the presence of weak electron localization in narrow inversion layers has been established beyond question.

VI. SUMMARY AND CONCLUSIONS

The primary objective of this work was to verify the existence of the quantum correction to the resistance due to weak localization of electrons in Al films and wires and to better understand these corrections in terms of microscopic mechanisms. In this section, we summarize the important developments in our understanding. We discuss our results in two parts, for thin films and for narrow wires.

A. Thin films

Our experiments on thin Al films provide strong quantitative support to the theory of localization in superconductors above T_c. The existence of superconducting fluctuations above the transition temperature of Al presents an interesting (and in some ways useful) complication in the data analysis. The study of magnetoresistance (in perpendicular magnetic fields) has been helpful is separating the effects due to weak localization and Maki-Thompson fluctuations from the other quantum effects. This separation is simple only in low $R_\square$ films such as we have studied.

A significant outcome of this work is the understanding of the inelastic mechanisms that destroy the phase coherence essential for localization. From our magnetoresistance measurements, we have clearly identified the inelastic mechanisms as three-dimensional electron-phonon scattering and two-dimensional electron-electron scattering. In addition, we find satisfactory agreement between the values of the inelastic scattering rates determined in superconductivity experiments (such as quasiparticle charge imbalance and microwave enhancement of the superconducting gap) and those from our localization experiments. We have also verified the scaling of the spin-orbit scattering time with the elastic scattering time, in agreement with the theory of Abrikosov and Gorkov. However, a quantitative understanding of spin-orbit scattering in terms of the material composition has not been possible. Other aspects of the experimental behavior of Al films are found to be in good order. The temperature dependence of resistance, $R(T)$, in thin films is very well explained by the theory. This provides valuable self-consistency checks to the magnetoresistance analysis and to the inferred inelastic rates. The experimentally observed contribution of electron-phonon scattering to $R(T)$ is consistent (based on a simple model) with the magnitude of the electron-phonon scattering inferred from magnetoresistance. Also, the magnetoresistance of thin films in parallel magnetic fields is in satisfactory agreement with the theory. Finally, we find that experiments performed on Al films in the various laboratories of the world do agree with each other, and support our interpretation of the electron inelastic rate. The mechanism(s) causing spin-orbit scattering in granular films does, in general, appear to differ from that in clean films.

B. Narrow wires

According to the original 1D theory of Thouless (which should apply in the limit of negligible spin-orbit scattering and magnetic scattering), the localization dimensionality is decided by the inelastic scattering length l_i. Spin-orbit scattering is significant even for Al, and we have therefore extended the localization theory to include spin-orbit scattering. As a result, we have introduced another length scale, l_2, for the 1D localization experiments. We have also evaluated the magnetoresistance contribution due to Maki-Thompson fluctuations in the one-dimensional case (when the sample width is smaller than l_i). Only when $(W,d) < l_i$ and l_2 is the sample in the fully-one-dimensional limit for its localization behavior. When $d < (l_i, l_2)$ but $l_2 < W < l_i$ the sample will show a mixed dimensional (1D+2D) behavior.

Our experimental study of narrow wires of width $W \sim 0.2$ μm have verified our theoretical predictions for

one-dimensional localization that includes spin-orbit scattering and superconducting fluctuations. The inferred values of l_i and $l_{s.o.}$ from these experiments show that $(W,d) < l_i$ and l_2, so that we do indeed meet (self-consistently) the conditions for 1D behavior. Further, we find quantitative agreement between the values for l_i inferred from the wires and the thin films of comparable quality. We do not see any evidence for a change in the dimensionality of the inelastic scattering mechanisms as sample width is reduced to ~ 0.2 μm. Finally we find that the crossover in localization dimensionality does indeed occur when the sample width is comparable to l_i, as predicted by Thouless. In a previous work,[11] we have reanalyzed the early experiments on 1D localization. We conclude that in most of those experiments 1D localization was not observed due to various complications in the sample material parameters and/or analyses. More recent experiments[75–77] fully support our results and the 1D localization theory.

A number of scientific issues still remain to be explored with localization studies. In the case of quench-condensed metal films, τ_i^{-1} has been observed[3] to go as T^2. This result indicates the possibility of distinctly different mechanisms in dirty films ($\rho \sim 100$ $\mu\Omega$ cm) as compared to those seen in our samples. Studies of the inelastic scattering mechanisms in such systems could lead to a better understanding of the metal-insulator transition.[81] Also, a systematic study of the effects of magnetic impurities on localization may be able to shed light on issues raised in the previous Kondo studies on metallic systems. In conclusion, we have demonstrated experimentally the existence of electron localization in Al films in the presence of superconducting fluctuations. Our experiments on 2D films have yielded understandable inelastic scattering rates. Furthermore, we have also shown that localization behavior in Al observed by the other researchers is also consistent with our results. In the case of 1D systems, our results are a *clear confirmation* of the localization theory. The theory must be generalized to include spin-orbit scattering. We have shown that a consistent interpretation of the experimental data in two- and one-dimensional systems for localization behavior is now possible.

Note added. Since the submittal of this manuscript, Wind *et al.*[82] have reported magnetoresistance measurements on Al and Ag wires sufficiently narrow to be in the one-dimensional regime for electron-electron scattering which fully confirm the predictions of Eq. (16) regarding magnitude, temperature dependence and width dependence. This new result, along with the earlier results on wider wires discussed in Sec. IV B, confirm that $l_{\rm int} = [\hbar D / k_B T]^{1/2}$ is the relevant dimensional length scale for electron-electron scattering.

ACKNOWLEDGMENTS

We thank B. J. Dalrymple and M. J. Rooks for assistance in the data analysis and A. Pooley for assistance with the scanning electron microscopy. We thank E. Abrahams, H. Fukuyama, J. M. Gordon, Y. Imry, W. E. Lawrence, J. M. B. Lopes dos Santos, W. L. McLean, A. Schmid, and J. W. Serene for useful discussions. This research was supported by the National Science Foundation (NSF) Grant Nos. DMR-17957 and DMR-8207443. The x-ray lithography system was supported in part by NSF Grant No. ECS-7927165.

APPENDIX

In this Appendix we clarify some confusion in the literature regarding the prefactor in the theoretical result for one-dimensional localization viz. Eq. (8b). The choice of this prefactor is important, since it can affect the inferred values of l_i and $l_{s.o.}$ when fitting Eq. (8b) to experimental results.

In his original derivation of the weak localization correction to the fractional change in resistance in one dimension (in the absence of spin dependent scattering and external magnetic field), Thouless[1(b)] obtained

$$\frac{\Delta R^{\rm loc}}{R}(T,H=0) = \frac{\rho_0}{A}\frac{(4\tau_i D)^{1/2}}{R_T} ,$$

with A the cross sectional area of the wire and R_T estimated to be 36.5 kΩ. We find an algebraic error in this estimate and note that based on Eq. (9) and Eq. (10) of Ref. 1(b), R_T should correspond to $2\pi\hbar/e^2$. Hence,

$$\frac{\Delta R^{\rm loc}}{R}(T,H=0) = \frac{\rho_0}{A}\frac{(4\tau_i D)^{1/2}}{2\pi\hbar/e^2} = \frac{R_\square}{\pi\hbar/e^2}\left[\frac{H_W}{H_i}\right]^{1/2} ,$$

where we have used our definition of H_W and H_i. This is in agreement with the prefactor in Eq. (8b).

We also note that in his alternate derivation of the weak localization correction,[1(a)] Thouless used $\sigma = \frac{1}{2} N(E_F) e^2 D$ for the Einstein relation, instead of the more commonly used $\sigma = N(E_F) e^2 D$. σ is the conductivity and $N(E_F)$ is the density of states at the Fermi energy per unit volume.

There is an additional source of confusion in the prefactor due to Alt'shuler *et al.*[20] They had obtained

$$\frac{\Delta R^{\rm loc}}{R}(T,H) = \frac{R_\square}{\pi^2\hbar/e^2}\left[\frac{H_W}{H_i}\right]^{1/2}\left[1+\frac{H^2}{48 H_i H_W}\right]^{-1/2}$$

in their evaluation of the conductivity. The additional π in the denominator is due to an algebraic error, and the authors have corrected the error in a more recent publication.[16]

We note that the experiments reported in this paper and those in Refs. 75 and 76 seem to indicate the choice of the prefactor in Eq. (8b) as correct through other consistency checks for the inferred fitting parameters.

*Current address: IBM T.J. Watson Research Center, Yorktown Heights, NY 10598.

[1]D. J. Thouless, (a) Phys. Rev. Lett. **39**, 1167 (1977); (b) Phys. Rep. **67**, 5 (1980), and Solid State Commun. **34**, 683 (1980).

[2]E. Abrahams, P. W. Anderson, D. C. Licciardello, and T. V. Ramakrishnan, Phys. Rev. Lett. **42**, 673 (1979).

[3]G. Bergmann, Phys. Rep. **107**, 1 (1984); P. A. Lee and T. V. Ramakrishnan, Rev. Mod. Phys. **57**, 287 (1985).

[4]R. C. Dynes, Physica (Utrecht) **109&110B**, 1857 (1982).

[5]B. L. Alt'shuler, A. G. Aronov, and P. A. Lee, Phys. Rev. Lett. **44**, 1288 (1980).

[6]B. L. Alt'shuler, A. G. Aronov, A. I. Larkin, and D. E. Khmel'nitskii, Zh. Eksp. Teor. Fiz. **81**, 768 (1981) [Sov. Phys.—JETP **54**, 411 (1981)]; B. L. Alt'shuler, D. E. Khmel'nitskii, A. I. Larkin, and P. A. Lee, Phys. Rev. B **22**, 5142 (1980); P. A. Lee and T. V. Ramakrishnan, *ibid.* **26**, 4009 (1982).

[7](a) A. I. Larkin, Pis'ma Zh. Eksp. Teor. Fiz. **31**, 239 (1980) [JETP Lett. **31**, 219 (1980)]; (b) J. M. B. Lopes dos Santos and E. Abrahams, Phys. Rev. B **31**, 172 (1985); (c) W. L. McLean and T. Tsuzuki, *ibid.* **29**, 503 (1984).

[8]P. Santhanam, and D. E. Prober, Phys. Rev. B **29**, 3733 (1984).

[9]P. Santhanam, S. Wind, and D. E. Prober, in *Proceedings of the Seventeenth International Conference on Low Temperature Physics, Karlsruhe, Federal Republic of Germany,* edited by U. Eckern, A. Schmid, W. Weber, and H. Wuhl (North-Holland, Amsterdam 1984), Part I, p. 495.

[10]P. Santhanam, S. Wind, and D. E. Prober, Phys. Rev. Lett. **53**, 1179 (1984).

[11]D. E. Prober, S. Wind, and P. Santhanam, in *Localization, Interaction and Transport Phenomena in Impure Metals,* Vol. 61 of *Springer Series on Solid State Sciences,* edited by B. Kramer, G. Bergmann, and Y. Bruynseraede (Springer-Verlag, Berlin, 1985), p. 148.

[12]P. Santhanam, Ph.D. thesis, Yale University, 1985. (Available from University Microfilms, Ann Arbor, MI 48106.)

[13]G. Bergmann, Phys. Rev. B **29**, 6114 (1984).

[14]H. Fukuyama, in *Percolation, Localization and Superconductivity,* edited by A. M. Goldman and S. Wolf (Plenum, New York, 1984), p. 161.

[15]P. W. Anderson, J. Phys. Chem. Solids, **11**, 26 (1959); J. Appel and A. W. Overhauser, Phys. Rev. B **29**, 99 (1984).

[16]B. L. Alt'shuler, A. G. Aronov, D. E. Khmel'nitskii, and A. I. Larkin, in *Quantum Theory of Solids,* edited by I. M. Lifshitz (Mir, Moscow, 1982).

[17]B. R. Patton, Phys. Rev. Lett. **27**, 1273 (1971).

[18]N. W. Ashcroft and N. D. Mermin, *Solid State Physics* (Holt, Rinehart and Winston, New York, 1976).

[19]S. Hikami, A. I. Larkin, and Y. Nagaoka, Prog. Theor. Phys. **63**, 707 (1980); S. Maekawa and H. Fukuyama, J. Phys. Soc. Jpn. **50**, 2516 (1981).

[20]B. L. Alt'shuler and A. G. Aronov, Pis'ma Zh. Eksp. Teor. Fiz. **33**, 515 (1981) [JETP Lett. **33**, 499 (1981)].

[21]M. E. Gershenson, B. N. Gubenkov, and Yu. E. Zhuravlev, Zh. Eksp. Teor. Fiz. **83**, 2348 (1982) [Sov. Phys.—JETP **56**, 1362 (1982)].

[22]D. Saint-James and P. G. de Gennes, Phys. Lett. **7**, 306 (1963).

[23]J. M. Gordon and J. B. Hansen, Phys. Rev. B **32**, 6039 (1985).

[24]N. Wiser, Contemp. Phys. **25**, 211 (1984).

[25]G. Bergmann, Z. Phys. B **48**, 5 (1982).

[26]W. E. Lawrence and A. B. Meador, Phys. Rev. B **18**, 1154 (1978); see Table II and Eq. (25): The rate relevant for delocalization is τ_i^{-1} at the Fermi surface [A. Schmid and H. Fukuyama (private communication)] as one should average only over an energy shell near E_F of $\Delta E = \hbar/\tau_i$ and this ΔE is much smaller than $k_B T$. To obtain Eq. (13), we use the rate given in Ref. 26, Table II and include the effective mass enhancement due to electron-phonon coupling.

[27]J. M. Ziman, *Electrons and Phonons* (Clarendon, Oxford, 1960), p. 213; A. B. Pippard, Philos. Mag. **46**, 1104 (1955).

[28]A. Schmid, in *Localization, Interaction and Transport Phenomena in Impure Metals,* Ref. 11, p. 212; Z. Phys. **259**, 421 (1973).

[29]A. Schmid, Z. Phys. **271**, 251 (1974).

[30]H. Takayama, Z. Phys. **263**, 329 (1973).

[31]Yu. Kagan and A. P. Zhernov, Zh. Eksp. Teor. Fiz. **50**, 1107 (1966) [Sov. Phys.—JETP **23**, 737 (1966)].

[32](a) W. E. Lawrence and J. W. Wilkins, Phys. Rev. B **7**, 2317 (1973); (b) A. H. MacDonald, Phys. Rev. Lett. **44**, 489 (1980).

[33]E. Abrahams, P. W. Anderson, P. A. Lee, and T. V. Ramakrishnan, Phys. Rev. B **24**, 6783 (1981).

[34]J. M. B. Lopes dos Santos, Phys. Rev. B **28**, 1189 (1983).

[35]B. L. Alt'shuler and A. G. Aronov, Solid State Commun. **46**, 429 (1983).

[36]H. Fukuyama and E. Abrahams, Phys. Rev. B **27**, 5976 (1983).

[37]B. L. Alt'shuler, A. G. Aronov, and D. E. Khmel'nitskii, J. Phys. C **15**, 7367 (1982).

[38]W. E. Eiler, J. Low. Temp. Phys. **56**, 481 (1984).

[39]H. Fukuyama, J. Phys. Soc. Jpn. **53**, 3299 (1984).

[40]E. Abrahams, in *Localization and Metal-Insulator Transitions,* edited by H. E. Fritzsche and D. Adler (Plenum, New York, 1985).

[41]W. Brenig, M-C. Chang, E. Abrahams, and P. Wolfle, Phys. Rev. B **31**, 7001 (1985); W. Brenig, J. Low. Temp. Phys. **60**, 297 (1985).

[42]J. L. Black, and B. L. Gyorffy, and J. Jackle, Philos. Mag. B **40**, 331 (1979).

[43](a) N. Giordano, W. Gilson, and D. E. Prober, Phys. Rev. Lett. **34**, 725 (1979); N. Giordano, Phys. Rev. B **22**, 5635 (1980); in *Proceedings of the International Conference on Physics in One Dimension,* edited by J. Bernasconi and T. Schneider (Springer-Verlag, Berlin, 1980); (b) J. T. Masden and N. Giordano, Physica (Utrecht) **107B**, 3 (1981).

[44]A. Abrikosov and L. P. Gor'kov, Zh. Eksp. Teor. Fiz. **42**, 1088 (1962) [Sov. Phys.—JETP **15**, 752 (1962)].

[45]R. Meservey and P. M. Tedrow, Phys. Lett. **58A**, 131 (1976); Phys. Rev. Lett. **41**, 805 (1978).

[46]J. E. Crow, M. Strongin, and A. K. Bhatnagar, Phys. Rev. B **9**, 135 (1974).

[47]D. E. Prober, in *Percolation, Localization and Superconductivity,* Ref. 14, p. 231.

[48]D. E. Prober, M. D. Feuer, and N. Giordano, Appl. Phys. Lett. **37**, 94 (1980).

[49]D. C. Flanders, Ph.D. thesis, Massachusetts Institute of Technology, 1978 (unpublished); D. C. Flanders and H. I. Smith, J. Vac. Sci. Technol. **15**, 995 (1978).

[50]Alfa Products, Danvers, Mass. 01923.

[51]R. D. Mathis Company, Long Beach, CA 90806.

[52]M. D. Feuer, Ph.D. thesis, Yale University, 1980. (Available from University Microfilms, Ann Arbor, MI 48106.)

[53]Model 147, Keithley Instruments, Inc., Cleveland, Ohio 44139.

[54]Linear Research Inc., San Diego, CA 92110.

[55]B. J. Dalrymple, Ph.D. thesis, Yale University, 1983. (Available from University Microfilms, Ann Arbor, MI 48106.) B. J. Dalrymple and D. E. Prober, Rev. Sci. Instrum. **55**, 958 (1984).

[56]M. Tinkham, *Introduction to Superconductivity* (McGraw-Hill, New York, 1975); From p. 266, the formula used to find the diffusion constant for a thin film is $D=(4k_Bc/e)(dH_{c2\perp}/dT)^{-1}$.

[57]E. Fawcett in Fermi Surface, edited by W. Harrison and M. B. Webb (Wiley, New York, 1960); also when the free electron Fermi velocity is divided by mass enhancement of 1.4 one obtains $\approx 1.3\times 10^8$ cm/sec.

[58]J. M. Gordon, Ph.D. thesis, Harvard University, 1984.

[59]C. C. Chi and J. Clarke, Phys. Rev. B **19**, 4495 (1979).

[60]J. M. Gordon, C. J. Lobb, and M. Tinkham, Phys. Rev. B **28**, 4046 (1983); *ibid.* **29**, 5232 (1984).

[61]P. C. van Son, J. Romijn, T. M. Klapwijk, and J. E. Mooij, Phys. Rev. B **29**, 1503 (1984).

[62]J. E. Mooij and T. M. Klapwijk, in *Localization, Interaction and Transport Phenomena in Impure Metals,* Ref. 11, p. 233.

[63]K. K. Choi, Phys. Rev. B **28**, 5774 (1983); R. A. Davies and M. Pepper, J. Phys. C **16**, L353 (1983).

[64]W. E. Lawrence and J. W. Wilkins, Phys. Rev. B **6**, 4466 (1972).

[65]G. Bergmann and C. Horriar-Esser, Phys. Rev. B **31**, 1161 (1985); P. E. Lindelof and S. Wong, Phys. Rev. B **33**, 1478 (1986).

[66]Y. Bruynseraede, M. Gijs, C. van Haesendonck, and G. Deutscher, Phys. Rev. Lett. **50**, 277 (1983); Helv. Phys. Acta **56**, 37 (1983) (and private communication).

[67]M. E. Gershenson, V. N. Gubankov, and Yu. E. Zhuravlev, Solid State Commun. **45**, 87 (1983); see caption of Fig. 1 for their data-fitting procedure; Zh. Eksp. Teor. Fiz. **85**, 287 (1983) [Sov. Phys.—JETP, **58**, 167 (1983)].

[68]B. Shinozaki, T. Kawaguti, and Y. Fujimori, J. Phys. Soc. Jpn. **53**, 3303 (1984).

[69]K. C. Mui, P. Lindenfeld, and W. L. McLean, Phys. Rev. B **30**, 2951 (1984); *Proceedings of the International Conference on Localization, Interaction and Transport Phenomena in Impure Metals* (Suppl.), edited by L. Schweitzer and B. Kramer (PTB, Braunschweig, 1984), p. 78.

[70]P. Chaudhari and H.-U. Habermeier, Phys. Rev. Lett. **44**, 40 (1980); Solid State Commun. **34**, 687 (1980); P. Chaudhari, A. N. Broers, C. C. Chi, R. Laibowitz, E. Spiller, and J. Viggiano, Phys. Rev. Lett. **45**, 930 (1980).

[71]A. E. White, M. Tinkham, W. J. Skoçpol, and D. C. Flanders, Phys. Rev. Lett. **48**, 1752 (1982).

[72]A. C. Sacharoff, R. M. Westervelt, and J. Bevk, Phys. Rev. B **29**, 1647 (1984).

[73]D. R. Overcash, B. A. Ratnam, M. J. Skove, and E. P. Stillwell, Phys. Rev. Lett. **44**, 1348 (1980).

[74]J. T. Masden and N. Giordano, Phys. Rev. B **31**, 6395 (1985).

[75]J. M. Gordon, Phys. Rev. B **30**, 6770 (1984).

[76]J. C. Licini, G. J. Dolan, and D. J. Bishop, Phys. Rev. Lett. **54**, 1585 (1985).

[77]J. J. Lin and N. Giordano, Phys. Rev. B **33**, 1519 (1986).

[78]H. Godfrin, P. Averbach, and M. Laviron, *Proceedings of the International Conference on Localization, Interaction and Transport Phenomena in Impure Metals,* Ref. 69, p. 336.

[79]R. G. Wheeler, K. K. Choi, A. Goel, R. Wisnieff, and D. E. Prober, Phys. Rev. Lett. **49**, 1674 (1982).

[80]W. J. Skoçpol, L. D. Jackel, E. L. Hu, R. E. Howard, and L. A. Fetter, Phys. Rev. Lett. **49**, 951 (1982).

[81]R. C. Dynes, J. P. Garno, G. B. Hertel, and T. P. Orlando, Phys. Rev. Lett. **53**, 2437 (1984).

[82]S. Wind, M. J. Rooks, V. Chandrasekhar, and D. E. Prober, Phys. Rev. Lett. **57**, 633 (1986).